

Stochastic geometry of critical curves, Schramm-Loewner evolutions, and conformal field theory

Ilya A. Gruzberg

The James Franck Institute, The University of Chicago
5640 S. Ellis Avenue, Chicago, IL 60637 USA

August 9, 2006

Abstract

Conformally-invariant curves that appear at critical points in two-dimensional statistical mechanics systems, and their fractal geometry have received a lot of attention in recent years. On the one hand, Schramm [1] has invented a new rigorous as well as practical calculational approach to critical curves, based on a beautiful unification of conformal maps and stochastic processes, and by now known as Schramm-Loewner evolution (SLE). On the other hand, Duplantier [2, 3] has applied boundary quantum gravity methods to calculate exact multifractal exponents associated with critical curves.

In the first part of this paper I provide a pedagogical introduction to SLE. I present mathematical facts from the theory of conformal maps and stochastic processes related to SLE. Then I review basic properties of SLE and provide practical derivation of various interesting quantities related to critical curves, including fractal dimensions and crossing probabilities.

The second part of the paper is devoted to a way of describing critical curves using boundary conformal field theory (CFT) in the so-called Coulomb gas formalism. This description provides an alternative (to quantum gravity) way of obtaining the multifractal spectrum of critical curves using only traditional methods of CFT based on free bosonic fields.

Contents

1	Introduction	4
2	Critical 2D systems and critical curves	6
3	Conformal maps and Loewner equation	11
4	Schramm-Loewner evolution	17
5	Basic results from stochastic calculus	22
5.1	Stochastic differential equations, Itô integrals and martingales	22
5.2	Itô formula	24
5.3	Stopping times and Dynkin formula	25
5.4	Backward and forward Kolmogorov equations	27
5.5	Feynman-Kac formula	28
5.6	Conditional probabilities and expectation values	29
6	Basic properties of SLE	30
6.1	Scaling	30
6.2	Phases on SLE	31
6.2.1	Transition at $\kappa = 4$	31
6.2.2	Transition at $\kappa = 8$	32
6.3	Locality	34
6.4	Restriction	37
7	Calculations with SLE	40
7.1	Left passage probability	40
7.2	Cardy's formula for crossing probability	43
7.3	Fractal dimensions of SLE curves	46
7.4	Derivative expectation	50
8	Critical curves and bosonic fields (Coulomb gas)	51
8.1	From loop models to bosonic fields	51
8.2	Coulomb gas CFT in the bulk	54
8.3	Coulomb gas CFT in the upper half plane	57
8.4	Creation of critical curves	59
9	Harmonic measure of critical curves	61
9.1	Definitions of harmonic measure	62
9.2	Moments of harmonic measure and multifractal spectrum	62

9.3	Critical curves and uniformizing maps	65
9.4	Derivative expectations and CFT in fluctuating geometry . .	67
9.5	Calculation of boundary multifractal exponents	69
9.6	Calculation of bulk multifractal exponents	72
10	Omitted topics: guide to the literature	74

1 Introduction

The area of two-dimensional (2D) critical phenomena has enjoyed a recent breakthrough. A radically new development, referred to as the Schramm (or stochastic) Loewner evolution (SLE) [1], has given new tools to study criticality in 2D, and also provided us with a new interpretation of the traditional conformal field theory (CFT) and Coulomb gas approaches. Examples of systems described by SLE include familiar statistical models — Ising, Potts, $O(n)$ model, polymers, — as well as “geometric” critical phenomena like percolation, self-avoiding random walks, spanning trees and others. The new description focuses directly on non-local structures that characterize a given system, be it a boundary of an Ising or percolation cluster, or loops in the $O(n)$ model. This description uses the fact that all these non-local objects become random curves at a critical point, and may be precisely characterized by stochastic dynamics of certain conformal maps.

The SLE approach is complementary to that of CFT, and the new description has not only reproduced many of the known results from previous approaches, but also gave new results, either conjectured before or unknown altogether. It appears that questions that are difficult to pose and/or answer within CFT are easy and natural in the SLE framework, and vice versa.

The SLE approach is very intuitive and transparent using traditional paradigms of stochastic processes — Brownian motion, diffusion, and the like. In spite of all this, SLE is not yet widely known in the physics community and deserves more attention and study. One goal of this paper is to give a brief introduction to this burgeoning field.

Another important recent advance (actually preceding the invention of SLE) in the study of critical 2D systems, has been the calculation of exact multifractal spectrum of critical clusters by Duplantier [2, 3], who has ingeniously applied methods of boundary quantum gravity (the KPZ formula of Ref. [4]). The second goal of this paper is to review Duplantier’s results and rederive them using traditional methods of CFT. To this end I to connect SLE with CFT in the so called Coulomb gas formulation. In this formulation the curves produced by SLE can be viewed as level lines of a height function (bosonic field) that fluctuates and is described by a simple Gaussian action with some extra terms. This formalism allows to perform a very transparent translation between SLE and CFT, and between geometric object (curves) and operators and states in the CFT.

Many reviews of SLE and its applications in physics already exist. They are listed in the references section in the end. Refs. [5]–[10] are geared for physicists, and Refs. [11]–[18] for mathematicians. My presentation

is for physicists who may want to read original mathematical papers on SLE. Therefore, I use mathematical language and notation, explaining and illustrating all important terms and ideas with plausible arguments and simple calculations. The presentation is not rigorous, but I try to formulate all important statements precisely. Another feature of this paper (mainly in its second part) is that I assume that readers are familiar with statistical mechanics and methods of CFT, some of which are briefly summarized in appropriate sections (see Ref. [19] for a thorough introduction).

The structure of the paper is as follows. In Section 2 I first describe microscopic origins of critical curves, as they appear in models of statistical mechanics defined on 2D lattices. Then I introduce various quantities of interest related to critical curves.

The next Section 3 presents some properties of conformal maps, especially those that map the complement of a curve in the upper half plane (UHP) to the UHP. These maps can be obtained as solutions of a simple differential equation introduced by Loewner. I provide a heuristic derivation of this equation and give a few examples of explicit solutions.

In Section 4 I introduce SLE and describe its basic properties (some of which are actually derived later) and relation to particular statistical mechanics models.

Section 5 provides a quick introduction to tools of stochastic analysis, the main ones being Itô formula and its consequences.

Basic properties of SLE, including its phases, locality and restriction, are considered and derived using stochastic calculus in Section 6.

In Section 7 I give several examples of non-trivial calculations within SLE, whose results provide probabilistic and geometric properties of critical curves. This section closes the part of the paper devoted to SLE.

The remaining sections, based on Refs. [20, 21], develop an alternative way of analyzing critical curves based on CFT methods in the Coulomb gas formalism.

The name “Coulomb gas” refers to a group of techniques that have been very fruitfully used to obtain exact critical exponents of various lattice models of statistical mechanics (see Ref. [22] for a review). A similar method was introduced by Dotsenko and Fateev [23] to reproduce correlations of the minimal models of CFT. The basic ingredient of all these methods is a bosonic action for a Gaussian free field. In Section 8 I show how lattice models can be related to the bosonic action, and how critical curves can be created by certain vertex operators.

Section 9 begins with definitions and properties of harmonic measure and its multifractal spectrum. The identification of curve-creating opera-

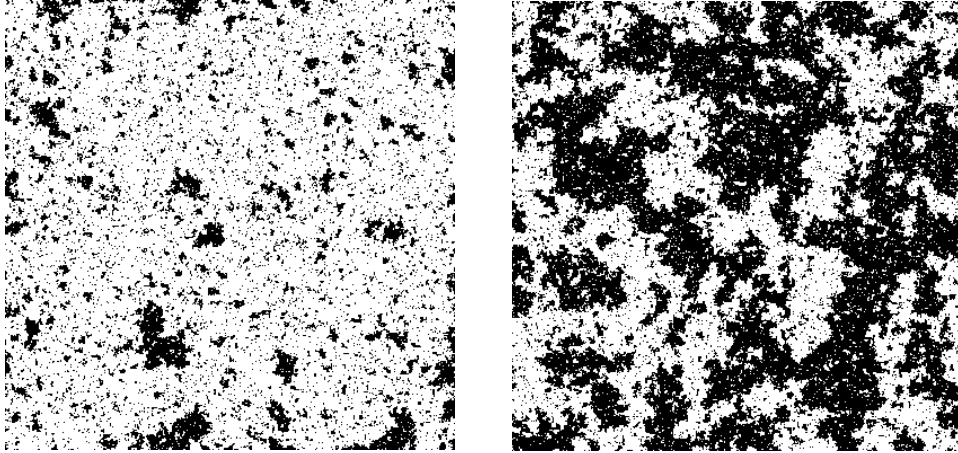


Figure 1: Ising clusters at low (left) and critical (right) temperature.

tors as vertex operators of Coulomb gas is used then to derive Duplantier’s results for many multifractal exponents characterizing stochastic geometry of critical curves.

The final Section 10 briefly lists topics related to SLE and its connection with CFT, that had to be omitted. This section may serve as a (necessarily incomplete) guide to the SLE literature.

2 Critical 2D systems and critical curves

Many very simple lattice models of statistical mechanics exhibit critical phenomena characteristic of continuous phase transitions. The prototype of all such models is the Ising model which describes the behavior of a collection of “spin” variables S_i located on sites of a lattice labeled by the index i , and taking values ± 1 . In this paper we will only consider two-dimensional models. In the Ising model the energy of the system is given by $H = -J \sum S_i S_j$, where the sum is over all nearest neighbor pairs of sites ij .

At a finite temperature T various possible spin configurations $\{S\}$ of the system have probabilities given by Gibbs distribution $e^{-H/T}/Z$, where the partition function is obtained by summing over all possible configurations: $Z = \sum_{\{S\}} e^{-H/T}$. Qualitative picture of this model is that at low temperatures the \mathbb{Z}_2 symmetry between the up ($S_i = 1$) and down ($S_i = -1$) directions of the spins is spontaneously broken, and the majority of spins points, say, up. As the temperature is increased, typical configurations in-

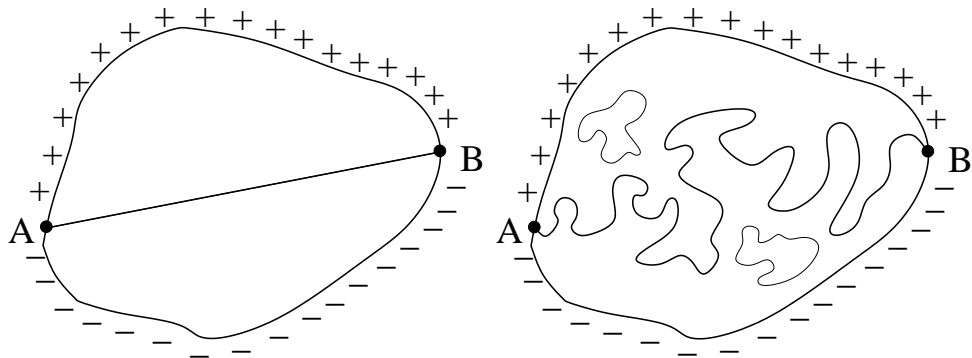


Figure 2: Domain walls in a finite Ising system. The boundary conditions change at points A and B , forcing a domain wall to go between these points. Left figure: zero temperature. Right figure: critical temperature.

volve small domains or connected clusters of down spins in the sea of up spins. The typical size of such clusters — the correlation length — increases indefinitely, as the temperature approaches a specific critical value T_c . At this temperature the clusters of up and down spins of all possible sizes are mixed together, and the whole picture is scale-invariant, see Fig. 1¹. The cluster boundaries or domain walls at the critical point are fractal curves that the SLE focuses on.

To be slightly more precise, let us consider a system in a simply connected region D with the boundary ∂D , with a very fine lattice inside (essentially, we want the lattice spacing to be much smaller than the system size and the correlation length at a given temperature), see Fig. 2. We can force a domain wall to go between two points A and B on the boundary ∂D . To this purpose let me impose the following boundary conditions. On the upper portion of the boundary between A and B we force the spins to be up, and on the lower portion — to be down. Then at zero temperature there will be exactly one straight domain wall between the points A and B . As the temperature increases, the domain wall will wander off the straight line, and eventually, at the critical temperature will become a complicated fractal curve. These curves will differ between the members of the statistical thermal ensemble, and will have particular weights or distribution within the ensemble.

Another prototypical example of a model that exhibits critical behavior

¹The applet that produced these pictures is available at <http://www.ibiblio.org/e-notes/Perc/contents.htm>

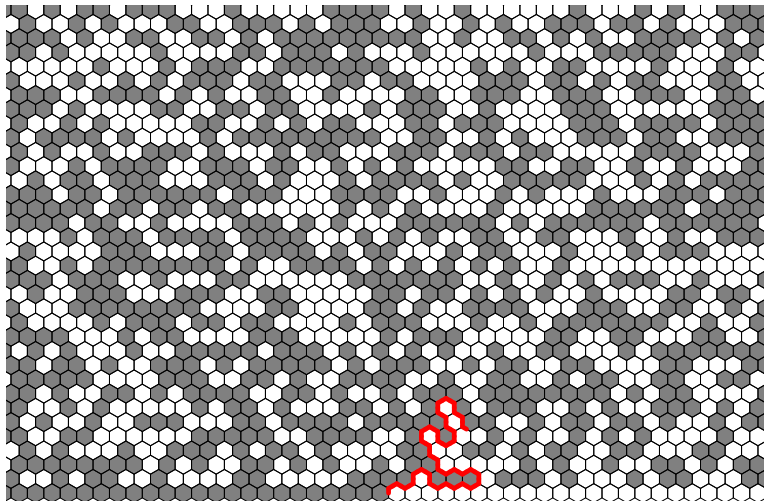


Figure 3: Critical percolation on a triangular lattice with a boundary condition that forces a domain wall (percolation hull) between the origin and infinity. The figure is borrowed from Ref. [17].

is the site percolation. In this model each site on a lattice is independently colored grey with probability p or white with probability $1 - p$. For each lattice there is a critical value $p = p_c$ such that an infinite connected cluster of grey sites appears in the system (that is, for $p < p_c$ all the gray clusters are finite). For a triangular lattice p_c is known to be exactly $1/2$. A good graphical representation of the critical site percolation on a triangular lattice is obtained if we replace every lattice point by a hexagon whose vertices lie on the dual honeycomb lattice. Then we can again force a domain wall into the system by making hexagons grey and white on two adjacent portions of the boundary. The Fig. 3 (borrowed from Ref. [17]) shows the upper half plane tiled with such hexagons. All the hexagons to the left of the origin on the horizontal axes (this is the boundary) are colored grey, and all the hexagons to the right are colored white. This produces a domain wall separating grey and white hexagons the beginning of which is shown in Fig. 3. Fig. 4 shows a much bigger system with the same boundary conditions.

Both the Ising and percolation models can be included in a larger class of models, loosely called the loop models, since their partition functions can be written as sums over loop configurations \mathcal{L} , either on the original or some related (the dual or the surrounding) lattice. Mappings between specific lattice models and loop models are described in detail in many reviews

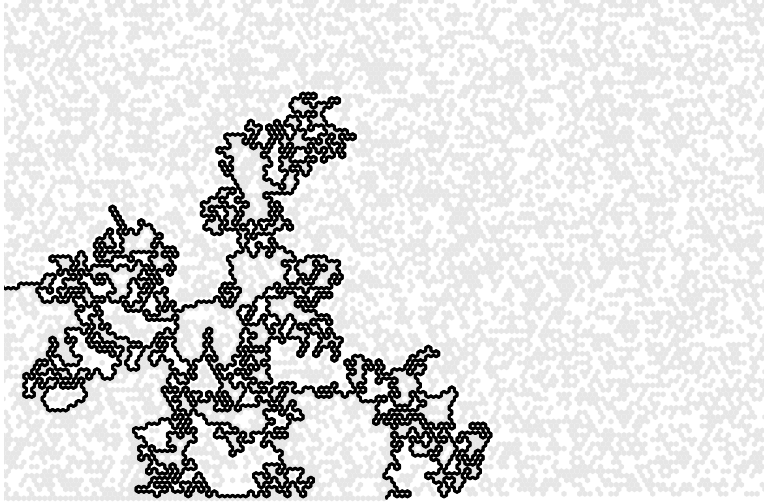


Figure 4: A long percolation hull. The figure is borrowed from Ref. [17].

[22, 24, 25, 26]. Here I only mention the $O(n)$ model because of the richness of its phase diagram. The model is defined in the simplest way on the honeycomb lattice directly in terms of closed loops:

$$Z_{O(n)} = \sum_{\mathcal{L}} x^L n^N. \quad (1)$$

Here x is the variable related to the temperature, L is the total length of all loops and N is their number in the configuration \mathcal{L} .

It is known from various approaches that the $O(n)$ model has a critical point at some value $x_c(n)$ for all n in the range $-2 \leq n \leq 2$. At the critical point the mean length of a loop diverges, but loops are dilute in the sense that the fraction of the vertices visited by the loops is zero. For $x > x_c(n)$ the loops are still critical but now visit a finite fraction of the sites. This is called the dense phase of the loop model. Finally, at zero temperature ($x = \infty$) the loops go through every point on the lattice, and this is called the fully packed phase.

For some values of the parameter n the $O(n)$ model is related to other known statistical mechanics models: $n = 2$ corresponds to the XY model, the limit $n = 0$ describes self-avoiding walks or polymers, and $n = -2$ corresponds to the so-called loop-erased random walk. The dense phase of the $O(n)$ model is also related to the critical point of the q -states Potts model. The Potts critical point exists for all $0 \leq q \leq 4$, and at that point

the boundaries of the so-called Fortuin-Kasteleyn clusters that appear in the high-temperature expansion of the q -states Potts model, are essentially the same as the loops in the dense phase of the $O(n)$ model with $n = \sqrt{q}$.

In all the models mentioned above, one can choose boundary conditions so as to introduce an open curve starting at one point on the boundary of a domain and ending at another boundary point. The continuum limit of these open curves with fixed ends on the boundary is exactly what is being studied using SLE.

One crucial paradigm in the study of critical phenomena is that of conformal invariance [27, 28]. For the critical curve described above this means that if we map conformally the region D in which our system is defined into another region D' , then the statistical weights or the distribution of the critical curves will be invariant under such mapping. In other words, any two curves that map into each other will have the same weight in the corresponding thermal ensembles. Then we can study these curves in a standard simple region, which we choose here to be the upper half plane \mathbb{H} with point A at the origin and point B at infinity.

In this setup we may ask various questions about the critical curves. Some of them are geometric. For example, we may want to know the fractal dimension of a critical curve. More generally, we can imagine that the cluster surrounded by a critical curve is charged, and then the charge distribution on the domain boundary will be very uneven or “lumpy”. This lumpiness is characterized by what is known as the spectrum of multifractal exponents. More precise definition uses the notion of the harmonic measure of the cluster boundary, and is explained in Section 9.

Another class of possible questions is probabilistic. We may ask about the probability that the critical curve between the origin and the infinity in \mathbb{H} passes to the left of a given point. Another question asks for the probability of the critical curve to touch the boundary at certain places in certain order. This is related to the so-called crossing probability in percolation that is defined as the probability for a connected cluster to span the critical system between two disjoint segments of the boundary. Sometimes we are interested only in the asymptotic behavior of probabilities of such events for long times or large spatial distances. These asymptotic probabilities behave in a power law fashion with some universal exponents that need to be found.

SLE provides an easy way of answering the above geometric and probabilistic questions and computing the corresponding quantities. In the following sections I will introduce the necessary tools from the theory of conformal maps and stochastic processes and will describe some calculations with SLE.

3 Conformal maps and Loewner equation

Consider the upper half plane $\mathbb{H} = \{z : \text{Im}z > 0\}$, with a curve γ starting at the origin on the real axis such that $\gamma \in \mathbb{H} \cup \{0\}$. We parametrize the curve by a real variable $t \in [0, \infty)$, and denote a point on γ as $\gamma(t)$ and (closed) segments as $\gamma[t_1, t_2]$.

A segment $\gamma[0, t]$ is an example of the so-called hull. A **hull** $K \subset \overline{\mathbb{H}}$ is a bounded subset of $\overline{\mathbb{H}}$ such that $\mathbb{H} \setminus K$ is simply connected and $K = \overline{K} \cap \overline{\mathbb{H}}$. So, a hull is, essentially, a bounded (but not necessarily connected) set bordering on the real line \mathbb{R} . By Riemann's mapping theorem (see Ref. [29]), for each such hull there is a conformal map g_K that maps $\mathbb{H} \setminus K$ to \mathbb{H} . Since conformal automorphisms of \mathbb{H} are Möbius transformations with real coefficients, we can make g_K unique by fixing three real parameters. A conventional "hydrodynamic" normalization is such that

$$\lim_{z \rightarrow \infty} (g_K(z) - z) = 0, \quad (2)$$

or, equivalently, that near $z = \infty$ the map has the form

$$g_K(z) = z + \sum_{n=1}^{\infty} \frac{a_n}{z^n}. \quad (3)$$

If the hull K is located a finite distance away from the origin, then $g_K(z)$ is regular at $z = 0$. In this situation it is more convenient for some purposes (see Sections 6.3, 6.4 below) to consider the map $\Phi_K(z) = g_K(z) - g_K(0)$, normalized as

$$\Phi_K(0) = 0, \quad \Phi_K(\infty) = \infty, \quad \Phi'_K(\infty) = 1, \quad (4)$$

Since the function $g_K(z)$ takes real values on the boundary of $\mathbb{H} \setminus K$, the coefficients $a_n \in \mathbb{R}$. The coefficient $a_1 = a(K)$ is called the half-plane capacity (or simply capacity) of the hull K . For any $r > 0$ the map $g_K(z)$ satisfies the scaling relation $g_{rK}(z) = r g_K(z/r)$, which implies the scaling for the capacity

$$a(rK) = r^2 a(K), \quad \forall r > 0. \quad (5)$$

Thus the capacity has the dimension of area. Geometrically, it is bounded above by R^2 , where R is the radius of the smallest semicircle that completely encloses the hull K .

Conformal maps for hulls can be composed as shown in Figure 5. Note that the mapping region monotonically shrinks under such a composition,

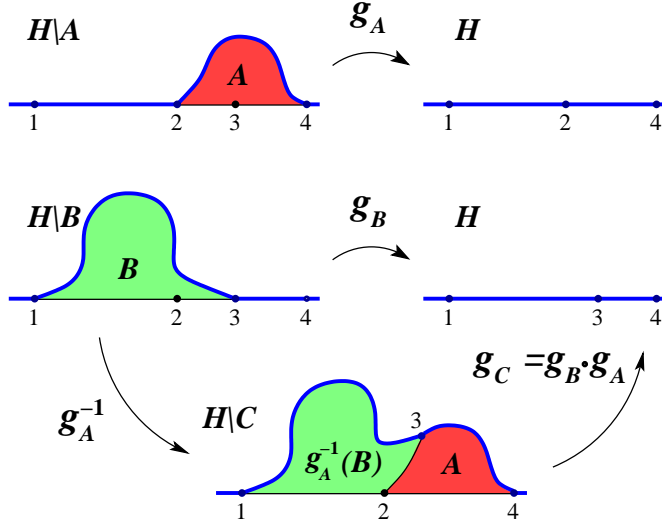


Figure 5: The composition of conformal maps. Here we denote $C = A \cup g_A^{-1}(B)$.

and the hulls grow. Their capacities satisfy another important property (additivity or composition rule):

$$a(A \cup g_A^{-1}(B)) = a(A) + a(B), \quad (6)$$

which can be easily checked by composing the conformal maps g_A and g_B in the form of Laurent expansions (3) and finding the coefficient a_1 of the composed map.

Consider now the map $g_{\gamma[0,t]} = g_t$ for the hull that is a segment of a curve, as in the beginning of this section. We can always choose the parametrization for the curve in such a way that

$$a(\gamma[0, t]) = 2t. \quad (7)$$

We will call the parameter t “time”, since the evolution of g_t in this variable will be of importance. Then it can be shown that the map g_t satisfies a very

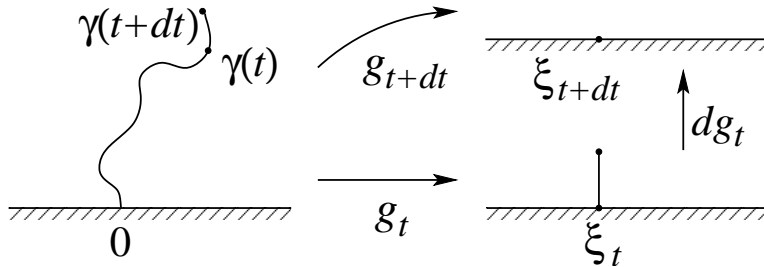


Figure 6: Illustration for the derivation of Loewner equation.

simple differential equation called Loewner equation [30]²:

$$\partial_t g_t(z) = \frac{2}{g_t(z) - \xi_t}, \quad g_0(z) = z, \quad (8)$$

where ξ_t is a real function that is the image of the tip of the cut $\gamma(t)$ under the map g_t :

$$\xi_t = g_t(\gamma(t)).$$

Let me give an intuitive derivation of this equation. Suppose that we already know the map g_t and want to find out what happens during the time increment between t and $t + dt$. Using the composition of maps we write $g_{t+dt} = dg_t \circ g_t$. This composition is illustrated in Fig. 6. Under the map g_t the segment $\gamma[t, t + dt]$ is mapped to a (almost) straight short vertical segment beginning at point $\xi_t \in \mathbb{R}$. Using the additivity property, Eq. (6), the capacity of this little segment is

$$a(g_t(\gamma[t, t + dt])) = 2dt. \quad (9)$$

The corresponding conformal map dg_t removing the segment is elementary:

$$dg_t(w) = \xi_t + \sqrt{(w - \xi_t)^2 + 4dt}. \quad (10)$$

²This equation has a fascinating history. It was invented in 1923 by Karl Löwner (who later changed his name to Charles Loewner, see more about him at <http://www-gap.dcs.st-and.ac.uk/~history/Mathematicians/Loewner.html>) to partially solve a famous conjecture from the theory of univalent functions proposed by Bieberbach in 1916. After many partial successes, the conjecture was finally proved by de Branges in 1985. The key element of the proof was the same Loewner equation! A very readable account of this story and the proof is given in Ref. [31].

Composing this with g_t and expanding in small dt we get

$$\begin{aligned} g_{t+dt}(z) &= dg_t(g_t(z)) = \xi_t + \sqrt{(g_t(z) - \xi_t)^2 + 4dt} \\ &\approx g_t(z) + \frac{2dt}{g_t(z) - \xi_t}. \end{aligned}$$

This immediately leads to Loewner equation (8) in the limit $dt \rightarrow 0$.

There are two ways in which one can think about Loewner equation. The first one was just presented: given a curve γ in the upper half plane, we can obtain, at least in principle, the real function ξ_t in the equation by constructing the corresponding conformal maps. The second way is the opposite: given a real continuous “driving” function ξ_t we can plug it into Loewner equation and solve it forward in time starting with the initial condition $g_0(z) = z$. It is known that the solution exists, but does not necessarily describe a map from \mathbb{H} cut along a segment of a curve. In some cases the hull that corresponds to the solution g_t contains two-dimensional regions of the upper half plane, as one of the examples below shows.

In general, the hull generated by the solution of Eq. (8) is defined as follows. For a given point $z \in \overline{\mathbb{H}}$, the solution of Eq. (8) is well defined as long as $g_t(z) - \xi_t \neq 0$. Thus, we define τ_z as the first time τ such that $\lim_{t \nearrow \tau} (g_t(z) - \xi_t) = 0$. For some points in $\overline{\mathbb{H}}$ the time $\tau_z = \infty$, meaning that at these points the Loewner map is defined for all times. The union of all the points z for which $\tau_z \leq t$ is the hull corresponding to the map $g_t(z)$:

$$K_t = \{z \in \overline{\mathbb{H}} : \tau_z \leq t\},$$

and its complement $H_t = \{z \in \mathbb{H} : \tau_z > t\} = \mathbb{H} \setminus K_t$ is the domain of g_t , that is the set of points for which $g_t(z)$ is still defined.

Another useful notion is that of the **trace** γ produced by Loewner equation. This is defined as the union points

$$\gamma(t) = \lim_{z \rightarrow 0} g_t^{-1}(z + \xi_t), \quad (11)$$

where the limit is taken within the upper half plane. Note that the trace and the hull are not necessarily the same objects, as we will see in a simple example below, and especially in the case of SLE_κ for some values of the parameter κ (see Section 6.2). The reason for this is that points may enter the growing hull in two different ways. Some of them are added to the trace itself, but others are swallowed, or enclosed by the trace “inside” the hull, see examples below.

One can exhibit many explicit solutions of the Loewner equation for several forms of the driving function ξ_t , see Ref. [32]. I will give here two

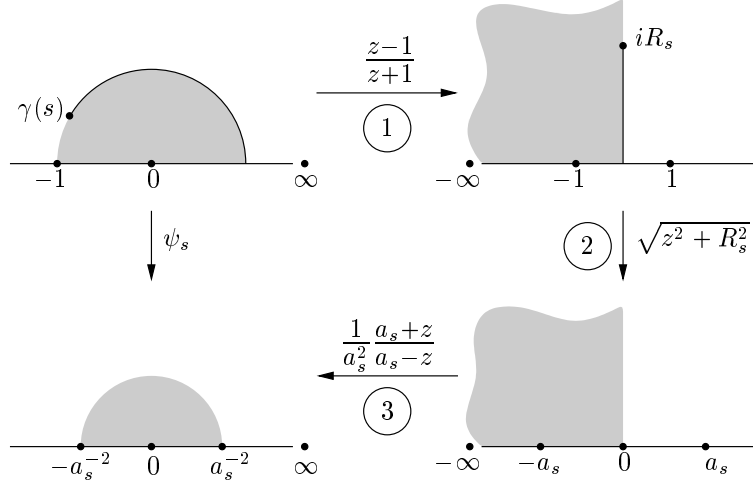


Figure 7: The sequence of maps for the construction of the function $g_s(z)$ in Eq. (12). The figure is borrowed from Ref. [32].

of them as illustrations. If $\xi_t = c$ is a constant, the solution of Eq. (8) is simply

$$g_t(z) = c + \sqrt{(z - c)^2 + 4t}.$$

The corresponding hull is the vertical straight segment between c and $c + 2i\sqrt{t}$. In this case the map g_t can be found by elementary means.

Another straightforward but instructive example described in detail in Refs. [32, 33] deals with a circular arc of radius r growing in the complex z plane from the point r on the real axis towards the point $-r$. The segment of this arc spanning the angle $s \in [0, \pi)$ is mapped to an interval on the imaginary axis $[0, iR_s]$, where $R_s = \tan(s/2)$, by the Möbius transformation $z_1 = (z - r)/(z + r)$, and then removed by the transformation from the previous example: $z_2 = \sqrt{R_s^2 + z_1^2}$. Further Möbius transformations are necessary to satisfy the hydrodynamic normalization (2). This leads to the mapping

$$g_s(z) = \frac{r}{a_s^2} \left(\frac{a_s + z_2}{a_s - z_2} + 2 - 2a_s^2 \right), \quad (12)$$

where $a_s^2 = 1 + R_s^2 = 1/\cos^2(s/2)$. The first three conformal maps in this sequence for $r = 1$ are illustrated in Fig. 7.

Expanding the function $g_s(z)$ near $z = \infty$ we find the capacity of the arc to be $2t = r^2(1 - a_s^{-4})$. After the reparametrization of the arc and the map

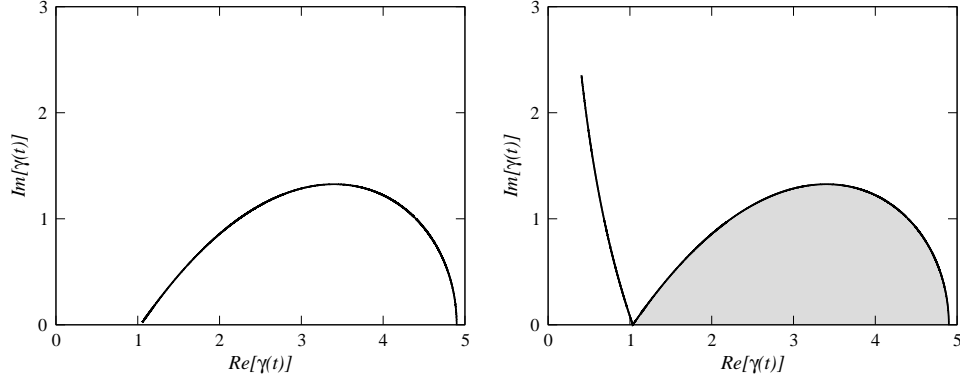


Figure 8: The trace and the hull for a touching event. Here $\xi_t = 2\sqrt{6(1-t)}$ for $t \in (0, 1)$ and zero elsewhere. Left shows the situation just before touching ($t \rightarrow 1^-$); right shows the situation after ($t > 1$). The trace is the thick dark line. The hull consists of that line plus the grey area. That area is added to the hull at $t = 1$. Note that there is a continuum of points added to the hull at the time of touching, but only one of these, $\gamma(1)$, is on the trace and is not swallowed. The figure is borrowed from Ref. [34].

g_s in terms of t we get the solution of Loewner equation

$$g_t(z) = \frac{(z-r)^2 + 2z\sqrt{r^2-2t} + (z+r)\sqrt{(z+r)^2 - 4z\sqrt{r^2-2t}}}{2z}, \quad (13)$$

corresponding to the driving function $\xi_t = 3\sqrt{r^2-2t} - 2r$. The branches of the square roots in Eq. (13) have to be chosen in such a way that

$$\lim_{t \rightarrow r^2/2} g_t(z) = \begin{cases} z + r^2/z, & \text{for } |z| \geq r, \\ -2r, & \text{for } |z| < r. \end{cases}$$

Note that at time $\tau = r^2/2$ the map g_t changes discontinuously. At any time before that the hull of the map is the segment of the arc. But exactly at $t = \tau$ the whole region $D = \{|z| < r, \text{Im } z \geq 0\}$ (the upper half of the disc of radius r) is mapped to the point $-2r$: all the points in this region are swallowed!

Let me define this notion more rigorously. We say that a point $z \in \overline{\mathbb{H}}$ is swallowed if $z \notin \gamma[0, \infty)$ but $z \in K_t$ for some t . In other words, swallowed points do not lie on the trace, but get enclosed by the trace in the “interior” portions of the hull. The time when a point gets swallowed is called the swallowing time for this point.

The time $\tau = r^2/2$ is the swallowing time for the whole region D . At this time the hull of the evolution K_τ is the closed semi-disc \overline{D} , while the trace is still the semi-circular arc. One may continue the evolution with the driving function $\xi_t = 0$ for $t > r^2/2$, and the trace will continue to grow as a simple curve from the point $-r$ on the real axis, while the hull will be $K_t = \overline{D} \cup \gamma[r^2/2, t]$, the union of the semi-disc and the portion of the trace grown after time τ . Similar swallowing of a region is illustrated in Fig. 8 for $\xi_t = 2\sqrt{6(1-t)}$ for $t \in (0, 1)$ and zero elsewhere.

4 Schramm-Loewner evolution

The remarkable discovery of Schramm [1] was that one can study Loewner equation (8) with random driving functions and in this way obtain all possible ensembles of curves with conformally invariant probabilities. Motivated by the conformal invariance of interfaces in statistical mechanical models, Schramm had argued that the driving function ξ_t has to be a continuous stationary stochastic process with independent increments. This argument is well explained in the existing reviews, here I simply indicate the basic idea. First, if we want to produce a curve without branching or self-intersections, we need to have a continuous input ξ_t . Next, for the curves to possess a conformally-invariant distribution, the corresponding maps have to be composed of statistically independent infinitesimal maps of the form (10). Together with the reflection symmetry this leads to essentially unique choice of $\xi_t = \sqrt{\kappa}B_t$, where $\kappa > 0$, and B_t is the standard Brownian motion started at $\xi(0) = 0$ (that is, $W_t = dB_t/dt$ is the white noise with unit strength: $\langle \dot{W}_t \dot{W}_s \rangle = \delta(t-s)$). The resulting stochastic Loewner equation

$$\partial_t g_t(z) = \frac{2}{g_t(z) - \sqrt{\kappa}B_t}, \quad g_0(z) = z, \quad (14)$$

and the sequence of conformal maps that it produces came to be known as SLE_κ , where SLE stands for stochastic Loewner evolution or Schramm-Loewner evolution.

Notice that after assuming the hydrodynamic normalization (2) and the parametrization in terms of the capacity (7), κ is the only important parameter of SLE. As we will see shortly, it completely determines the properties of SLE, its hulls and traces.

Often a shifted version of $g_t(z)$ is introduced:

$$w_t(z) = g_t(z) - \xi_t, \quad w_0(z) = z.$$

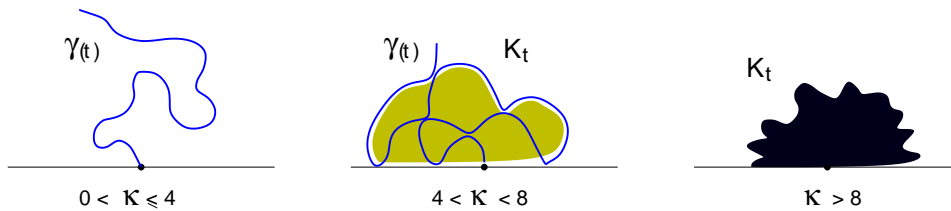


Figure 9: The phases of SLE. The figure is borrowed from Ref. [33].

This function satisfies the simple Langevin-type equation

$$\partial_t w_t(z) = \frac{2}{w_t(z)} - \sqrt{\kappa} \dot{B}_t, \quad w_0(z) = z. \quad (15)$$

It is the simplicity of this equation together with the powerful methods of the theory of stochastic processes that makes SLE a very versatile calculational tool. I will show how to do computations with it in the following sections. But first let me summarize the most important properties of SLE (some of them will be derived later in Section 6). These properties are quite non-trivial. Some of them have been rigorously formulated and established in Refs. [35].

- First of all, for all values of κ one can still define the trace of an SLE as the union of points $\gamma(t) = \lim_{z \rightarrow 0, z \in \mathbb{H}} w_t^{-1}(z)$ (and this limit exists). Moreover, the trace is a continuous curve starting at $\gamma(0) = 0$, reaching infinity as $t \rightarrow \infty$ and never crossing itself (self-avoiding).
- For $0 \leq \kappa \leq 4$ an SLE trace γ is a simple curve (does not have double points). In this case the SLE hull coincides with the trace: $K_t = \gamma[0, t]$, and no point in $\overline{\mathbb{H}}$ gets swallowed.
- For $4 < \kappa < 8$ an SLE trace has infinite number of double points. The trace sort of “touches” itself and the real axis at every scale. Every time such touching occurs, a whole finite region of the plane gets swallowed. As time goes on, almost all the points in $\overline{\mathbb{H}}$ (except the points on the trace) get swallowed.
- For $\kappa \geq 8$ the trace is a space-filling curve (a random analog of the Peano curve). This means that no point gets swallowed, but all the points in $\overline{\mathbb{H}}$ lie on the trace.

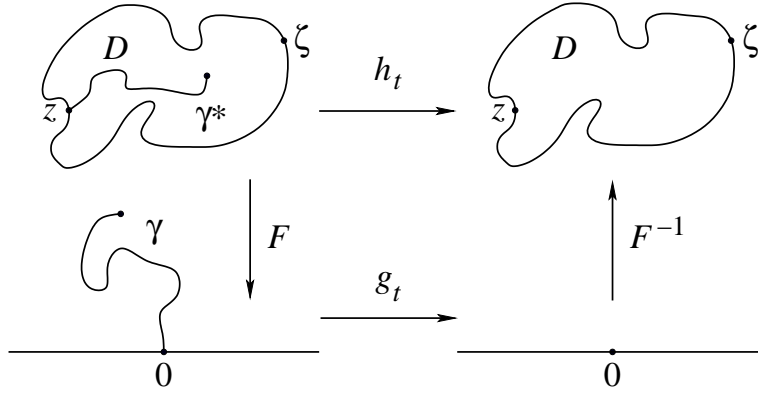


Figure 10: Definition of SLE in an arbitrary simply-connected domain D .

- The fractal dimension of the trace is (proven in Refs. [36, 37])

$$d_f(\kappa) = \begin{cases} 1 + \frac{\kappa}{8} & \text{for } \kappa \leq 8, \\ 2 & \text{for } \kappa \geq 8. \end{cases} \quad (16)$$

The different behaviors of traces and hulls of SLE for different values of κ may be called phases in analogy with statistical mechanics. These are schematically shown in Fig. 9.

A heuristic derivation of some of these properties given below in Section 6 will not be rigorous but will still require the use of probabilistic techniques. Therefore, in Section 5 I briefly summarize relevant results of stochastic calculus. Then in Section 7 I give examples of practical calculations with SLE, deriving a number of non-trivial critical exponents and scaling functions.

So far we have defined chordal SLE $g_t(z)$ and its traces and hulls only in the upper half plane \mathbb{H} . We can now map any simply-connected domain D to \mathbb{H} by a conformal transformation $F(z)$. We fix this function uniquely by requiring that

$$F(z) = 0, \quad F(\zeta) = \infty, \quad F'(\zeta) = 1, \quad (17)$$

where z and ζ are two distinct points on the boundary of D . Then, by definition, the chordal SLE in D from z to ζ is the family of maps $h_t(z) = F^{-1}(g_t(F(z)))$, with a possible random time change, see Fig 10. The trace of the new SLE is $\gamma^* = F^{-1}(\gamma)$, and the hulls are $K_t^* = F^{-1}(K_t)$.

Conformal invariance of SLE then means that, first of all, a trace γ^* in the domain D locally looks the same as a trace γ in \mathbb{H} . In particular, it

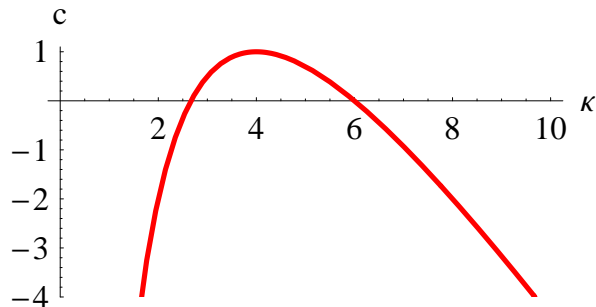


Figure 11: Central charge as a function of κ . Notice that κ and $\kappa' = 16/\kappa$ correspond to the same c . For example, for both $\kappa = 8/3$ and $\kappa = 6$ the central charge is zero. These values correspond to self-avoiding walks and boundaries of percolation clusters.

has the same fractal dimension. Secondly, various random events (crossings, swallowings, etc.) that correspond to each other under the map F , have the same probabilities. The requirement of such conformal invariance was crucial in the original definition of SLE.

Most importantly for applications in statistical mechanics, SLE produces conformally-invariant self-avoiding random traces that are statistically equivalent to critical curves in statistical mechanics models. It is actually very difficult to make this statement precise, and a lot of efforts has gone and is going into establishing the correspondence between SLE for different values of κ with critical points of various lattice models.

Correlation functions of local quantities at these critical points are described by CFTs with central charges $c \leq 1$. Bauer and Bernard [33] argued that SLE describes critical curves in all these CFTs. The relation between the SLE parameter κ and the central charge happens to be

$$c_\kappa = \frac{(8 - 3\kappa)(\kappa - 6)}{2\kappa} = 1 - 3\frac{(\kappa - 4)^2}{2\kappa}. \quad (18)$$

This function is plotted in Fig. 11. It possesses a remarkable duality, namely

$$c_\kappa = c_{\kappa'}, \quad \text{where} \quad \kappa' = \frac{16}{\kappa}. \quad (19)$$

Duplantier [2, 3] has argued that this duality has a geometric meaning. Namely, in the language of SLE, for $\kappa > 4$ an SLE_κ hull K_t has the boundary ∂K_t (also called external perimeter or frontier), which locally looks like an $\text{SLE}_{\kappa'}$ simple curve with fractal dimension $d_f(\kappa') = 1 + 2/\kappa$.

Lattice model	κ	c_κ	$d_f(\kappa)$	$d_f(\kappa')$	References
Loop-erased random walk	2	-2	5/4	-	[1, 38]
Self-avoiding random walk	8/3	0	4/3	-	[39]
Ising model spin cluster boundaries	3	1/2	11/8	-	[35]
Dimer tilings	4	1	3/2	-	[35, 40]
Harmonic explorer	4	1	3/2	-	[41]
Level lines of Gaussian field	4	1	3/2	-	[42]
Ising model FK cluster boundaries	16/3	1/2	5/3	11/8	[35]
Percolation cluster boundaries	6	0	7/4	4/3	[1, 43, 44]
Uniform spanning trees	8	-2	2	5/4	[38]

Table 1: Some lattice models for which a correspondence with SLE has been conjectured or rigorously established. The dash in the $d_f(\kappa')$ column means that the hull and the trace are the same.

Notice that the central charge vanishes for $\kappa = 8/3$ and $\kappa = 6$. These values are special from SLE point of view, since for these values the SLE hulls possess very special properties called locality and restriction, correspondingly. We will consider these properties in Sections 6.3, 6.4.

Many different arguments, including comparison of critical exponents, have lead to correspondences between SLE_κ and specific lattice models that we summarize in the Table 1. All these models can be related either to the critical point or the dense phase of the $O(n)$ model, or to the critical point of the q -states Potts model. The Coulomb gas methods map these models to a Gaussian bosonic field theory with coupling constant g and with background and screening charges. Within this theory one can identify the curve creating operators and establish a relation between g and κ . As a result, we get the following relations between the parameters n , q , g and κ :

$$n = -2 \cos \pi g, \quad g = \frac{4}{\kappa}, \quad 2 \leq \kappa \leq \infty, \quad (20)$$

$$q = 2 + 2 \cos 2\pi g, \quad g = \frac{4}{\kappa}, \quad 4 \leq \kappa \leq 8. \quad (21)$$

Mathematically rigorous formulation of conjectures related to general Potts and $O(n)$ models can be found in Refs. [15, 35].

The critical points of $O(n)$ model correspond to the range $2 \leq \kappa \leq 4$ ($1 \leq g \leq 2$), while the dense phase is described by $\kappa \geq 4$ ($0 \leq g \leq 1$). Parts of these ranges correspond to negative n . The critical point of the Potts

model is the same as the dense phase of the $O(n)$ model with $n = \sqrt{q}$ only for positive n , which explains the restriction on κ in Eq. (21). All these relations are reviewed below in Section 8.

Results presented in Section 8 allow us to arrive at detailed geometric description of critical curves by calculating the spectrum of multifractal exponents of the harmonic measure. These exponents include and generalize the fractal dimension $d_f(\kappa)$ (16). This is done in Section 9.

5 Basic results from stochastic calculus

To analyze SLE and apply it to the study of critical curves, we need to use stochastic calculus. This section provides a brief summary of the necessary techniques.

Here we only consider one-dimensional stochastic processes. As an example it is useful to keep in mind a simple diffusion of a particle on an interval (a, b) on the real line. Everything trivially generalizes to higher dimensions.

All the material in this section and much more is very nicely presented in Refs. [45, 46].

5.1 Stochastic differential equations, Itô integrals and martingales

A stochastic differential equation (SDE) is, essentially, a Langevin equation, which mathematicians like to write in terms of differentials:

$$dx_t = u(x_t, t) dt + v(x_t, t) dB_t. \quad (22)$$

Here the first term in the right-hand side is called the drift term, and in the second term B_t is the standard Brownian motion (BM) started at $B_0 = 0$ (that is, $W_t = dB_t/dt$ is the white noise with unit strength). The process x_t describes a random “trajectory” of a Brownian particle. The simplest example is

$$dx_t = \sqrt{\kappa} dB_t.$$

This describes a simple diffusion with the diffusion coefficient κ .

BM is a Gaussian process with independent increments: for any set of times $0 \leq t_1 < t_2 < \dots < t_k$ the random variables

$$B_{t_1}, B_{t_2} - B_{t_1}, \dots, B_{t_k} - B_{t_{k-1}}$$

are independent and normally distributed with zero means and variances $t_1, t_2 - t_1$, etc. We note here that from this definition it can be shown that all of the following are standard BMs:

$$\begin{array}{lll}
-B_t, & & \text{reflection invariance,} \\
B_{s+t} - B_s, & \forall s, t > 0, & \text{time homogeneity,} \\
a^{-1}B_{a^2t}, & \forall a > 0, & \text{scaling,} \\
tB_{1/t}, & & \text{time inversion.}
\end{array} \tag{23}$$

One can write the solution of Eq. (22) as

$$x_t = x_0 + \int_0^t u(x_s, s) ds + \int_0^t v(x_s, s) dB_s.$$

The last term here is an **Itô integral** defined as the limit of finite sums

$$\sum_i v(x_{s_i}, s_i)(B_{s_{i+1}} - B_{s_i}).$$

Note the important property that the integrand is taken always at the left end of the time interval. Then it is always independent from the increment of the BM multiplying the integrand. This means that upon averaging over B_t all the terms in the above sum vanish. The same is true then for the Itô integral:

$$\mathbf{E}^x \left[\int_0^t v(x_s, s) dB_s \right] = 0. \tag{24}$$

Here $\mathbf{E}^x[\dots]$ stands for the expectation value, or the average over the realizations of B_t , and the superscript x refers to the initial condition $x_0 = x$. Similarly, we have the following Itô isometry:

$$\mathbf{E}^x \left[\left(\int_0^t v(x_s, s) dB_s \right)^2 \right] = \mathbf{E}^x \left[\int_0^t v^2(x_s, s) ds \right].$$

The previous two equations imply another very important property of the Itô integral, namely, that it is a martingale. **Martingale** is, essentially, a stochastic process M_t which satisfies the following properties:

$$\begin{array}{ll}
\mathbf{E}[|M_t|] < \infty, & \forall t, \\
\mathbf{E}[M_t \mid \text{history of } M \text{ up to } s] = M_s, & \forall t \geq s.
\end{array}$$

The second condition (which is formalized using the notion of filtration of σ -algebras \mathcal{M}_t to describe “the history of M ”) contains a conditional expectation value (see Section 5.6), and it means that if we know that at some time s the process M has the value M_s , then the expectation value of this process in the future at any moment $t \geq s$ is going to be the same M_s independently of time t . In particular, the unconditional expectation value $\mathbf{E}[M_t] = M_0$ is simply given by the initial value of the martingale. Martingales necessarily satisfy stochastic differential equations without drift terms:

$$dM_t = v(M_t, t) dB_t. \quad (25)$$

5.2 Itô formula

Next we need the so called Itô formula, which describes a change of variables in stochastic calculus. Let me formulate it for 1D processes first. Suppose that we have an Itô stochastic process x_t which satisfies the SDE

$$dx_t = u(x_t, t) dt + v(x_t, t) dB_t,$$

where B_t is the standard BM (that is, $W_t = dB_t/dt$ is the white noise with unit strength). Now we take any “reasonable” function $f(x, t)$ (it should be twice continuously differentiable in both arguments) and define $y_t = f(x_t, t)$. Then y_t is again an Itô process that satisfies the SDE

$$dy_t = \frac{\partial f(x_t, t)}{\partial t} dt + \frac{\partial f(x_t, t)}{\partial x_t} dx_t + \frac{1}{2} \frac{\partial^2 f(x_t, t)}{\partial x_t^2} (dx_t)^2.$$

Mnemonicly, we need to expand to first order in time, but to second order in x_t . The quantity $(dx_t)^2$ is found using the rules

$$(dt)^2 = dt dB_t = dB_t dt = 0, \quad (dB_t)^2 = dt.$$

Thus $(dx_t)^2 = v^2(x_t, t) dt$, and the SDE for y_t becomes the **Itô formula**:

$$\begin{aligned} dy_t = & \left(\frac{\partial f(x_t, t)}{\partial t} + \frac{1}{2} v^2(x_t, t) \frac{\partial^2 f(x_t, t)}{\partial x_t^2} + u(x_t, t) \frac{\partial f(x_t, t)}{\partial x_t} \right) dt \\ & + v(x_t, t) \frac{\partial f(x_t, t)}{\partial x_t} dB_t. \end{aligned} \quad (26)$$

Often one encounters “time-homogeneous” processes when both $u(x_t)$ and $v(x_t)$ do not depend explicitly on time. In this case the process x_t

is called a diffusion with drift $u(x_t)$ and diffusion coefficient $v^2(x_t)$. For a function $y_t = f(x_t)$ of a diffusion the previous formula slightly simplifies:

$$dy_t = \left(\frac{1}{2}v^2(x_t)\frac{d^2f(x_t)}{dx_t^2} + u(x_t)\frac{df(x_t)}{dx_t} \right) dt + v(x_t)\frac{df(x_t)}{dx_t} dB_t. \quad (27)$$

The coefficients here do not depend explicitly on t , which means that in this case the process y_t is also a diffusion. The differential operator \hat{A} appearing in the first term here is called the **generator** of the diffusion x_t :

$$\hat{A}f(x) = \frac{1}{2}v^2(x)\frac{d^2f(x)}{dx^2} + u(x)\frac{df(x)}{dx}.$$

we can integrate Eq. (27):

$$f(x_t) = f(x_0) + \int_0^t \hat{A}f(x_s) ds + \int_0^t v(x_s)\frac{df(x_s)}{dx_s} dB_s. \quad (28)$$

5.3 Stopping times and Dynkin formula

It is often interesting to study functions of stochastic processes at various random times. Such a random time τ is called a **stopping time** if at any moment t we can decide whether $\tau < t$ or not, or, in other words, whether τ has happened before time t . In our basic example we can consider, for example, the escape time, that is, the first time τ when the diffusing particle leaves the interval (a, b) :

$$\tau_{(a,b)} = \inf\{t : x_t \notin (a, b)\}. \quad (29)$$

In this example in each realization of our random process we are able to say whether the particle is in the interval at time t or outside it. Similarly, we can consider the first hitting time of a closed set $A \subset \mathbb{R}$:

$$\tau_A = \inf\{t : x_t \in A\}.$$

Now we evaluate Eq. (28) at some stopping time τ :

$$f(x_\tau) = f(x_0) + \int_0^\tau \hat{A}f(x_s) ds + \int_0^\tau v(x_s)\frac{df(x_s)}{dx_s} dB_s.$$

It can be shown that an analog of the martingale property (24) holds for Itô integrals with limits that are stopping times (this is related to the so-called strong Markov property of the BM, which states that even for a stopping

time τ the increment $B_{t+\tau} - B_\tau$ is a standard BM independent from B_t for $t \in [0, \tau]$. Then, taking the expectation values on both sides of the last equation we get the so-called **Dynkin formula**:

$$\mathbf{E}^x[f(x_\tau)] = f(x) + \mathbf{E}^x \left[\int_0^\tau \hat{A}f(x_s) ds \right]. \quad (30)$$

we assumed here that $x_0 = x$. Also, to really prove this formula, one needs to assume that $\mathbf{E}^x[\tau] < \infty$.

The Dynkin formula is extremely useful when we need to find various escape probabilities. Let me consider one example in detail. Suppose, we have a diffusion x_t started at $x_0 = x \in (a, b)$. Then at the exit time $\tau = \tau_{(a,b)}$ (see Eq. (29)) the particle can only escape the interval (a, b) either at the point a or at the point b . Then we can ask the question: “What is the probability that the escape happens through the point a ?” Formally, we need to find one of the quantities

$$P_a = \mathbf{P}[x_\tau = a], \quad P_b = \mathbf{P}[x_\tau = b],$$

where $\mathbf{P}[X]$ denotes the probability of the event X . It is obvious that these two probabilities add to one:

$$P_a + P_b = 1. \quad (31)$$

We will find another equation relating p_a and p_b using the Dynkin formula.

To do this, we consider the expectation value

$$\mathbf{E}^x[f(x_\tau)] = P_a f(a) + P_b f(b).$$

For any function $f(x_t)$ the LHS of this equation is given by the Dynkin formula. But if we find a function that satisfies the equation

$$\hat{A}f(x) = 0,$$

then the Itô formula (27) implies that $f(x_t)$ is a martingale (no drift term in the equation), and the Eq. (30) simplifies to $\mathbf{E}^x[f(x_\tau)] = f(x)$, and for such a function we get

$$P_a f(a) + P_b f(b) = f(x).$$

Combining this with Eq. (31), we finally find

$$P_a = \frac{f(x) - f(b)}{f(a) - f(b)}, \quad P_b = \frac{f(a) - f(x)}{f(a) - f(b)}. \quad (32)$$

Since \hat{A} is a linear differential operator, the function $f(x)$ can usually be found explicitly. Often it is expressed in terms of the hypergeometric function.

Let us note that to use the formulas (32), we need *any non-constant* zero mode of \hat{A} . There is a continuum of such solutions parametrized by two constants of integration (\hat{A} is a second order differential operator), but both the additive and the multiplicative constants cancel when a zero mode is substituted into Eq. (32).

5.4 Backward and forward Kolmogorov equations

Let us denote

$$b(x, t) = \mathbf{E}^x[f(x_t)].$$

Then taking \mathbf{E}^x of both sides in Eq. (28) and differentiating with respect to t , we get

$$\frac{\partial b}{\partial t} = \mathbf{E}^x[\hat{A}f(x_t)].$$

It turns out that the right hand side here can be expressed in terms of $b(x, t)$ also. Roughly speaking (this is not very trivial), the expectation value and the operator \hat{A} can be interchanged (after this \hat{A} acts on the variable x), giving the so called **backward Kolmogorov equation**:

$$\frac{\partial b}{\partial t} = \hat{A}b, \quad b(x, 0) = f(x). \quad (33)$$

Note that this is different from the more familiar Fokker-Planck equation. In fact, the Fokker-Planck equation (called the forward Kolmogorov equation in mathematics) involves the operator \hat{A}^* that is adjoint to \hat{A} :

$$\hat{A}^* f(x) = \frac{1}{2} \frac{d^2}{dx^2}(v^2(x)f(x)) - \frac{d}{dx}(u(x)f(x)).$$

The forward Kolmogorov equation involving \hat{A}^* appears as follows. The process x_t has the transition measure density $p_t(y, x)$, which means that the expectation values of functions of x_t can be found like this:

$$\mathbf{E}^x[f(x_t)] = \int f(y)p_t(y, x) dy.$$

This is equivalent to $p_t(y, x) = \mathbf{E}^x[\delta(x_t - y)]$, which is a familiar definition of the probability density for the process x_t . The density $p_t(y, x)$ is also

the kernel or the Green's function of the diffusion x_t . It is this function that satisfies the forward Kolmogorov equation with respect to the final coordinate y :

$$\frac{\partial}{\partial t} p_t(y, x) = \hat{A}_y^* p_t(y, x).$$

Because the operator \hat{A}^* has all the derivatives on the left, the total probability is conserved: $\int p_t(y, x) dy = \mathbf{E}^x[1] = 1$.

5.5 Feynman-Kac formula

A simple generalization of the backward Kolmogorov equation (33) is the so-called Feynman-Kac (FK) formula. It concerns the expectation value

$$c(x, t) = \mathbf{E}^x \left[\exp \left(- \int_0^t V(x_s) ds \right) f(x_t) \right],$$

where $V(x)$ is a continuous function such that the integral in the exponent converges as $t \rightarrow \infty$, $f(x)$ is as before, and x_t is a time-homogeneous Itô process (a diffusion). The FK formula is the following partial differential equation for $c(x, t)$:

$$\frac{\partial c}{\partial t} = \hat{A}c - Vc, \quad c(x, 0) = f(x). \quad (34)$$

This formula is obtained (schematically) as follows. We define

$$D_t(x) = \int_0^t V(x_s) ds, \quad C(x_t, t) = e^{-D_t(x)} f(x_t). \quad (35)$$

The process $C(x_t, t)$ explicitly depends on t through its first factor, and the Itô equation for it is obtained from the formula (22):

$$dC(x_t, t) = [\hat{A} - V(x_t)] C(x_t, t) dt + v(x_t) \frac{\partial C(x_t, t)}{\partial x_t} dB_t. \quad (36)$$

Upon averaging the last term vanishes, as usual, and we get

$$\frac{\partial c}{\partial t} = \mathbf{E}^x [(\hat{A} - V(x_t)) C(x_t, t)].$$

Similar to the case of the backward Kolmogorov equation, the right hand side can be expressed in terms of $c(x, t)$, which results in Eq. (34).

There is a variant of the FK formula that we can call a stationary FK formula. Namely, we can choose the function $f(x)$ in Eq. (35) to satisfy the stationary version of Eq. (34):

$$[\hat{A} - V(x)]f(x) = 0. \quad (37)$$

Then the process $C(x_t, t)$ defined in Eq. (35) with $f(x)$ being a solution of (37) is a martingale, since the drift term in the Itô formula (36) vanishes! The expectation value $c(x, t)$ is then really a function of x only, and is equal to $f(x)$ for all times.

Now if we know that the process x_t is transient, that is, $\lim_{t \rightarrow \infty} x_t = \infty$, we normalize $f(x)$ such that $f(\infty) = 1$, and denote $D(x) = D_\infty(x) < \infty$ we get

$$f(x) = \lim_{t \rightarrow \infty} \mathbf{E}^x[C(x_t, t)] = \mathbf{E}^x[e^{-D(x)}]. \quad (38)$$

It should be clear now that in this situation we can compute the characteristic function $\chi(k, x) = \mathbf{E}^x[e^{ikD(x)}]$ of the random variable D . In addition, if the variable $D(x)$ is known to be non-negative, the same approach gives the Laplace transform $L(s, x)$ of its probability distribution function $p(D, x)$:

$$L(s, x) = \mathbf{E}^x[e^{-sD(x)}] = \int_0^\infty e^{-sD(x)} p(D, x) dD. \quad (39)$$

Notice that all the quantities $D(x)$, $\chi(k, x)$, $L(s, x)$, and $p(D, x)$ implicitly depend on x , the initial value of the random process x_t .

5.6 Conditional probabilities and expectation values

Sometimes in the study of random variables and stochastic processes it is interesting or necessary to restrict the statistical ensemble of realizations to a sub-ensemble satisfying a certain condition. This condition may depend on the outcome of a certain random event. For example, for a diffusion on the real line we may consider only trajectories that always stay on the positive semi-axis, or the ones that happen to be on the positive semi-axis at a certain time. Such a restriction of an ensemble is called conditioning.

Within a restricted or conditioned ensemble we can ask for probabilities of various events or expectation values of random quantities. These are called conditional probabilities and expectation values. In words we can say: “What is the probability of an event A given that an event B happened?”

Such probability is denoted by $\mathbf{P}[A | B]$. It is well known in probability theory that conditional probabilities are easily calculated by the formula

$$\mathbf{P}[A | B] = \frac{\mathbf{P}[A \text{ and } B]}{\mathbf{P}[B]}, \quad (40)$$

where $\mathbf{P}[A \text{ and } B]$ is the unconditioned probability that the events A and B both happen, and $\mathbf{P}[B]$ is the unconditioned probability that the event B happens. Notice that the Eq. (40) only makes sense if the event B has non-zero probability $\mathbf{P}[B] > 0$.

Similarly, given that an event B occurs, we may want to find the expectation value of a random variable X , denoted $\mathbf{E}[X | B]$. Conditional expectation values have many known properties, but there is no general explicit formula for them similar to Eq. (40).

6 Basic properties of SLE

In this Section, based mainly on Refs. [35, 47, 48], we consider the basic properties of SLE. Some of them have already been mentioned, and they will be here illustrated by plausible arguments. These arguments already require some calculations typical for SLE. The main idea of most simple calculations with SLE is to look at various random events in the physical plane, then see what happens at the same time in the mathematical plane. Then we choose a simple real function of the SLE process and study the values this function assumes during the interesting events.

6.1 Scaling

The scaling property of the Brownian motion (23) immediately implies the scaling for the SLE processes $g_t(z)$ and the growing SLE hulls K_t . Namely, we have the following stochastic equivalence:

$$g_t(z) = \frac{1}{a}g_{a^2t}(az), \quad w_t(z) = \frac{1}{a}w_{a^2t}(az), \quad \text{in law.} \quad (41)$$

By this we mean that the random quantities on both sides of these equations have the same probability distribution. Eq. (41) is easily derived by observing that the SDE for the right hand side contains $\frac{\sqrt{\kappa}}{a}B_{a^2t}$ as the driving function. The scaling for the SLE processes (41) immediately implies a similar scaling for the SLE hulls:

$$K_t = \frac{1}{a}K_{a^2t} \quad \text{in law.} \quad (42)$$

6.2 Phases on SLE

The phases of SLE were already described above in Section 4. Here we provide a crude derivation of the phases and phase transitions between them.

6.2.1 Transition at $\kappa = 4$.

First we discuss the transition at $\kappa = 4$. To this end we will fix a point $x \in \mathbb{R}$ on the real axis in the physical plane and consider the motion of its image $x_t = w_t(x)$ up to the time when it hits 0 (which may never happen):

$$dx_t = \frac{2}{x_t} dt - \sqrt{\kappa} dB_t, \quad x_0 = x.$$

In the mathematical plane, we fix points a and b on the real axis so that

$$0 < a < x < b < \infty.$$

Let τ be the exit time from the interval $[a, b]$. Being continuous, the process x_t can exit $[a, b]$ either through a (with probability P_a), or through b (with probability $1 - P_a$). As described in Sec. 5.3, the probability P_a can be found if we know a non-constant zero mode $f(x)$ of the generator of diffusion x_t , see Eq. (32).

Now if we take the limits $a \rightarrow 0$, $b \rightarrow \infty$, it becomes the probability for x_t to hit 0 in a finite time, which is the probability for the point x on the physical plane to belong to the hull:

$$P = \lim_{b \rightarrow \infty} \lim_{a \rightarrow 0} \frac{f(x) - f(b)}{f(a) - f(b)}. \quad (43)$$

In general, the order of limits matters here. If it is reversed,

$$\tilde{P} = \lim_{a \rightarrow 0} \lim_{b \rightarrow \infty} \frac{f(x) - f(b)}{f(a) - f(b)} \quad (44)$$

is the probability for x_t to come arbitrarily close to 0, that is, for the hull to come arbitrarily close to the boundary. Note that in order to determine these probabilities, only the behavior of a zero mode of \hat{A} at zero and at infinity is necessary.

The generator for the process x_t is

$$\hat{A} = \frac{\kappa}{2} \frac{d^2}{dx^2} + \frac{2}{x} \frac{d}{dx}.$$

A non-constant zero mode of this operator is

$$f(x) = \begin{cases} |x|^{1-\frac{4}{\kappa}} & \text{for } \kappa \neq 4, \\ \log |x| & \text{for } \kappa = 4. \end{cases}$$

Substituting this into Eqs. (43, 44) we find that the answer is independent of x , thus the probability for the hull to touch the boundary

$$P = \begin{cases} 0 & \text{for } \kappa \leq 4, \\ 1 & \text{for } \kappa > 4. \end{cases}$$

For $\kappa = 4$ the order of limits is important and we find that

$$\tilde{P} = \begin{cases} 0 & \text{for } \kappa < 4, \\ 1 & \text{for } \kappa \geq 4. \end{cases}$$

These formulas clearly exhibit a sort of “phase transition” at $\kappa = 4$.

6.2.2 Transition at $\kappa = 8$.

This transition is more subtle. To study it, we fix two points $0 < x < y < \infty$ on the real axis in the physical plane, and compare the times τ_x and τ_y when they enter the growing SLE hull. For $\kappa > 4$ both these times are finite.

It happens that for $\kappa < 8$ there is a finite probability that the points x and y are swallowed simultaneously: $\mathbf{P}[\tau_x = \tau_y] > 0$. On the other hand, for $\kappa \geq 8$, with probability one, $\tau_x < \tau_y$. In this case the points on the real axis are added to the trace sequentially. The same is true for points in \mathbb{H} .

To make these statements plausible (without giving a real proof), let us consider $x_t = w_t(x)$, $y_t = w_t(y)$, and $q_t = \log \frac{y_t}{x_t}$. By continuity it is clear that $0 \leq x_t \leq y_t \leq \infty$ for all times, so $0 \leq q_t \leq \infty$.

If x joins the hull before y (that is, $\tau_x < \tau_y$), then $q_{\tau_x} = \infty$, and the probability $\mathbf{P}[q_{\tau_x} = \infty] > 0$ (as well as $\mathbf{P}[q_{\tau_x} = 0] > 0$). If the points x and y join the hull simultaneously, then q_t stays finite (bounded) for all times up to $\tau_x = \tau_y$, and $\mathbf{P}[q_{\tau_x} = \infty] = 0$. So we need to consider the motion of q_t .

Using Itô formula for q_t we get

$$dq_t = \frac{1}{y_t} dy_t - \frac{1}{x_t} dx_t - \frac{1}{2y_t^2} (dy_t)^2 + \frac{1}{2x_t^2} (dx_t)^2.$$

Here we need to substitute, as usual,

$$dx_t = \frac{2}{x_t} dt - \sqrt{\kappa} dB_t, \quad dy_t = \frac{2}{y_t} dt - \sqrt{\kappa} dB_t.$$

This gives the following SDE:

$$dq_t = \left(\frac{\kappa}{2} - 2\right) \left(\frac{1}{2x_t^2} - \frac{1}{2y_t^2}\right) dt + \sqrt{\kappa} \left(\frac{1}{x_t} - \frac{1}{y_t}\right) dB_t.$$

Notice that this equation is not of standard Itô type, since the coefficients of the right hand side depend separately on x_t and y_t , but not on q_t . This is easily remedied by a trick that is called “a random time change”.

This time change amounts to consider a new time variable

$$\tilde{t} = \int_0^t \frac{ds}{x_s^2},$$

which is a monotonous function of t (since we integrate a positive quantity x_s^{-2}). In differential form the time change is

$$d\tilde{t} = dt/x_t^2.$$

We also need to consider the stochastic process

$$\tilde{B}_t = \int_0^t \frac{dB_s}{x_s}, \quad d\tilde{B}_t = \frac{dB_t}{x_t}.$$

Notice that

$$(d\tilde{B}_t)^2 = (dB_t)^2/x_t^2 = dt/x_t^2 = d\tilde{t}.$$

Therefore, the process $B_{\tilde{t}} = \tilde{B}_t$ is the standard Brownian motion with respect to the new time \tilde{t} !

In terms of the new variables the SDE for $q_{\tilde{t}}$ takes the standard Itô form:

$$dq_{\tilde{t}} = \left(\frac{\kappa}{2} - 2\right) (1 - e^{-2q}) d\tilde{t} + \sqrt{\kappa} (1 - e^{-q}) dB_{\tilde{t}}.$$

The generator of diffusion for this process is

$$\hat{A} = \frac{\kappa}{2} (1 - e^{-q})^2 \frac{d^2}{dq^2} + \left(\frac{\kappa}{2} - 2\right) (1 - e^{-2q}) \frac{d}{dq},$$

and we need to find a zero mode of this operator to study the probability $\mathbf{P}[q_t = \infty]$.

The equation $\hat{A}f = 0$ can be easily solved by rewriting it as (prime denotes the derivative with respect to q)

$$\frac{f''}{f'} = (\log f')' = \left(\frac{4}{\kappa} - 1\right) \coth \frac{q}{2}.$$

When we integrate this equation, we can drop the integration constants, which are inessential, as was explained in the end of Section 5.3:

$$\log f' = \left(\frac{8}{\kappa} - 2\right) \log \left(\sinh \frac{q}{2}\right), \quad f' = \left(\sinh \frac{q}{2}\right)^{\frac{8}{\kappa}-2}.$$

Since we now only consider $\kappa > 4$, the function $f'(q)$ exponentially decays as $q \rightarrow \infty$, and we can choose (ignoring a multiplicative constant)

$$f(q) = \int_q^\infty \left(\sinh \frac{s}{2}\right)^{\frac{8}{\kappa}-2} ds.$$

When $q \rightarrow 0$, this integral converges at the lower limit when $\kappa < 8$, and in this case we get $\mathbf{P}[q_{\tau_x} = 0] > 0$. On the other hand, when $\kappa \geq 8$, the function $f(q)$ diverges as $q \rightarrow 0$, and $\mathbf{P}[q_{\tau_x} = 0] = 0$, implying that $\mathbf{P}[q_{\tau_x} = \infty] = 1$.

6.3 Locality

Many properties of SLE can be discovered by studying how SLE gets perturbed by distortions of the boundary of the domain where it evolves. Such distortions can be described by conformal maps. This setting is similar to the definition of SLE in an arbitrary simply-connected domain D in Section 4, but there are important differences.

Specifically, let us consider a usual SLE_κ evolving in the upper half plane. Consider a hull A located a finite distance away from the origin. Then the SLE trace may hit the hull and have a non-zero overlap with its interior. Note that this would not happen for SLE defined in the domain $\mathbb{H} \setminus A$ as in Section 4. Let the hitting time of the hull A be τ_A .

Next we consider the image of the SLE under the map Φ_A removing the hull A from the upper half plane and normalized as in Eq. (4):

$$\Phi_A(0) = 0, \quad \Phi_A(\infty) = \infty, \quad \Phi'_A(\infty) = 1, \quad (45)$$

The SLE hulls K_t get mapped to hulls $\tilde{K}_t = \Phi_A(K_t)$, and these can be removed from \mathbb{H} by the family of maps \tilde{g}_t . Though this procedure works for any value of κ , for simplicity we illustrate it in Fig. 12 for $\kappa \leq 4$, in which case SLE hulls are the traces. The maps \tilde{g}_t are normalized as

$$\tilde{g}_t(z) = z + \frac{a_t}{z} + o(z^{-1}), \quad z \rightarrow \infty,$$

where a_t is the capacity of \tilde{K}_t , and evolve according to the Loewner equation

$$\partial_t \tilde{g}_t(z) = \frac{\partial_t a_t}{\tilde{g}_t(z) - \tilde{\xi}_t}. \quad (46)$$

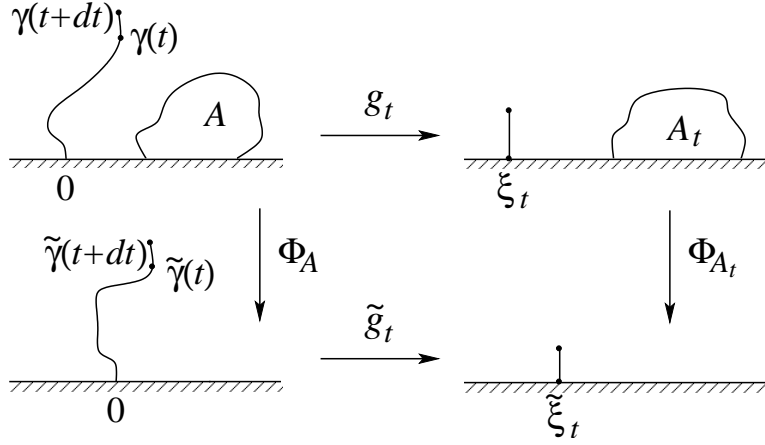


Figure 12: Various maps in the definitions of locality and restriction. Similar figure illustrating a commutative diagram of conformal maps first appeared in Ref. [48].

We want now to find the properties of the driving function $\tilde{\xi}_t$ and see if there is a time change that would make it a Brownian motion $\sqrt{\kappa}B_{\tilde{t}}$. If this is the case, then $\tilde{g}_t(z)$ is the standard SLE_κ , at least for $t \leq \tau_A$. This implies that the original $\text{SLE } g_t$ is the same as the SLE defined in the domain $\mathbb{H} \setminus A$ according to Section 4, see Fig. 10 and Eq. (17). Loosely speaking, we can say that in this situation the $\text{SLE } g_t$ does not feel the presence of the hull A until K_t hits A . This justifies the name **locality** for this property. As we will see next, this happens only for $\kappa = 6$, which was rigorously established in Ref. [47] (Ref. [48] contains a simpler proof that we follow here), and is in perfect agreement with the statement that SLE_6 describes the scaling limit of critical percolation interfaces. Even on the lattice such interfaces are determined locally, since every site is black or white independently of the others.

To find the capacity a_t and the driving function $\tilde{\xi}_t$ we notice that the hull $K_t \cup A$ can be removed by a different sequence of maps. Namely, we first remove the hull K_t of the original SLE by g_t . Doing this, we deform the hull A into a hull A_t . Next we remove the hull A_t by the map $\Phi_t = \Phi_{A_t}$ normalized the same way as Φ_A , see Fig. 12 where an infinitesimal step from t to $t + dt$ is also shown. Then we have a commutative diagram of maps, meaning that

$$\tilde{g}_t(\Phi_A(z)) = \Phi_t(g_t(z)). \quad (47)$$

In particular, for the image of the tip of the trace $\gamma(t)$ we have

$$\tilde{\xi}_t = \tilde{g}_t(\Phi_A(\gamma(t))) = \Phi_t(g_t(\gamma(t))) = \Phi_t(\xi_t), \quad (48)$$

where $\xi_t = \sqrt{\kappa}B_t$ is the usual SLE driving function.

From the derivation of Loewner equation in Section 3 we already know that the capacity of the infinitesimal vertical segment $g_t(\gamma[t, t + dt])$ is $2dt$, see Eq. (9). When this segment (together with the hull A_t) is mapped to \mathbb{H} by Φ_t , it simply gets rescaled by $\Phi_t'(\xi_t)$. (Note that the map Φ_t is regular away from the hull A_t , and in particular, at the point ξ_t . Also, since the map preserves a portion of the real axis near ξ_t , its derivative $\Phi_t'(\xi_t) > 0$). Therefore, the scaling property of the capacity, Eq. (5), implies

$$\partial_t a_t = 2\Phi_t'(\xi_t)^2. \quad (49)$$

Taking time derivative of Eq. (47) and using Eqs. (46, 49) we get

$$\frac{2\Phi_t'(\xi_t)^2}{\tilde{g}_t(\Phi_A(z)) - \tilde{\xi}_t} = \partial_t \Phi_t(g_t(z)) + \Phi_t'(g_t(z)) \frac{2}{g_t(z) - \xi_t}.$$

Denoting $w = g_t(z)$ and using Eq. (48) we simplify this to

$$\partial_t \Phi_t(w) = \frac{2\Phi_t'(\xi_t)^2}{\Phi_t(w) - \Phi_t(\xi_t)} - \frac{2\Phi_t'(w)}{w - \xi_t}.$$

The right hand side of this equation is non-singular in the limit $w \rightarrow \xi_t$. To see this we expand it in powers of $(w - \xi_t)$ (using Mathematica):

$$\partial_t \Phi_t(w) = -3\Phi_t''(\xi_t) + \left(\frac{1}{2} \frac{\Phi_t''(\xi_t)^2}{\Phi_t'(\xi_t)} - \frac{4}{3} \Phi_t'''(\xi_t) \right) (w - \xi_t) + O((w - \xi_t)^2). \quad (50)$$

The first term of the expansion gives $\partial_t \Phi_t(w)|_{w=\xi_t} = -3\Phi_t''(\xi_t)$.

Finally, using Itô formula for $\tilde{\xi}_t = \Phi_t(\xi_t)$, we have

$$\begin{aligned} d\tilde{\xi}_t &= \partial_t \Phi_t(w)|_{w=\xi_t} dt + \Phi_t'(\xi_t) d\xi_t + \frac{1}{2} \Phi_t''(\xi_t) (d\xi_t)^2 \\ &= \Phi_t'(\xi_t) d\xi_t + \left(\frac{\kappa}{2} - 3 \right) \Phi_t''(\xi_t) dt. \end{aligned}$$

For $\kappa = 6$ and only for this value the drift term in the above equation vanishes, and $d\tilde{\xi}_t$ becomes $\sqrt{\kappa}dB_{\tilde{t}}$ after the random time change $d\tilde{t} = \Phi_t'(\xi_t)^2 dt$, proving locality for SLE_6 .

6.4 Restriction

In this Section we consider the same setup as in the previous one, but only for $\kappa \leq 4$. In this case SLE traces are simple curves, and there is a non-zero probability $\mathbf{P}[\gamma \cap A = \emptyset]$ that a trace $\gamma[0, \infty)$ does not intersect the hull A . This is also the probability that the hitting time $\tau_A = \infty$. The collection of these probabilities for all hulls A located a finite distance away from the origin completely characterizes the distribution of the curve γ , since it determines the likelihoods for the curve to go through various places. As we will show in this Section, these probabilities can be found for $\text{SLE}_{8/3}$ in term of the map Φ_A normalized again as in Eq. (45).

Given that an SLE_κ trace does not intersect A , we can map the whole trace together with $\mathbb{H} \setminus A$ to \mathbb{H} by the map Φ_A and ask what the probability distribution of the image $\Phi_A(\gamma)$ is. If this distribution happens to be the same SLE_κ , we say that SLE_κ satisfies the **restriction** property. Following Ref. [48], where conformal restriction was introduced and rigorously studied, we will show below that this happens only for $\kappa = 8/3$.

We start by studying the rescaling factor $\Phi'_t(\xi_t)$ as a function of time. The second term in the expansion (50) leads to

$$\partial_t \Phi'_t(w)|_{w=\xi_t} = \frac{1}{2} \frac{\Phi''_t(\xi_t)^2}{\Phi'_t(\xi_t)} - \frac{4}{3} \Phi'''_t(\xi_t),$$

and then Itô formula gives

$$\begin{aligned} d\Phi'_t(\xi_t) &= \partial_t \Phi'_t(w)|_{w=\xi_t} dt + \Phi''_t(\xi_t) d\xi_t + \frac{1}{2} \Phi'''_t(\xi_t) (d\xi_t)^2 \\ &= \Phi''_t(\xi_t) d\xi_t + \left(\frac{1}{2} \frac{\Phi''_t(\xi_t)^2}{\Phi'_t(\xi_t)} + \left(\frac{\kappa}{2} - \frac{4}{3} \right) \Phi'''_t(\xi_t) \right) dt. \end{aligned}$$

The drift term in this equation cannot be removed by any choice of κ . However, if we apply Itô formula again to $M_t^{(h)} = \Phi'_t(\xi_t)^h$, we get

$$\begin{aligned} \frac{dM_t^{(h)}}{hM_t^{(h)}} &= \frac{d\Phi'_t(\xi_t)}{\Phi'_t(\xi_t)} + \frac{h-1}{2} \frac{[d\Phi'_t(\xi_t)]^2}{\Phi'_t(\xi_t)^2} \\ &= \frac{\Phi''_t(\xi_t)}{\Phi'_t(\xi_t)} d\xi_t + \left(\frac{(h-1)\kappa + 1}{2} \frac{\Phi''_t(\xi_t)^2}{\Phi'_t(\xi_t)^2} + \left(\frac{\kappa}{2} - \frac{4}{3} \right) \frac{\Phi'''_t(\xi_t)}{\Phi'_t(\xi_t)} \right) dt. \quad (51) \end{aligned}$$

If we now choose $\kappa = 8/3$ and $h = 5/8$, the drift term in the last equation vanishes, which implies that $M_t^{(5/8)}$ is a martingale. Then, on the one hand, the expectation value of $M_t^{(5/8)}$ is given by the value of this process at $t = 0$:

$$\mathbf{E}[M_t^{(5/8)}] = M_0^{(5/8)} = \Phi'_0(\xi_0)^{5/8} = \Phi'_A(0)^{5/8}.$$

On the other hand, let us consider the expectation value at the stopping time τ when the trace γ hits for the first time either the hull A or the semicircular arc C_R of radius R centered at the origin and completely enclosing A . The following argument is very similar to the application of Dynkin formula to diffusions on an interval in Section 5.3.

At time τ we have two options: either $\gamma(\tau)$ hits the hull A (in which case $\tau = \tau_A$) or it hits the arc C_R (in which case $\tau_A > \tau$). Then

$$\mathbf{E}[M_\tau^{(5/8)}] = \mathbf{P}[\tau = \tau_A] \Phi'_{\tau_A}(\xi_{\tau_A})^{(5/8)} + \mathbf{P}[\tau_A > \tau] \Phi'_\tau(\xi_\tau)^{(5/8)}.$$

In the first case the point ξ_{τ_A} hits a “side” of the hull A_{τ_A} (see Fig. 12) where the derivative $\Phi'_{\tau_A}(\xi_{\tau_A})$ vanishes. Thus, only the second option contributes to the expectation value $\mathbf{E}[M_\tau^{(5/8)}]$. Then if we take the radius R to be very large, the point ξ_τ becomes very far from the hull A_τ , and the derivative $\Phi'_\tau(\xi_\tau)$ tends to 1. Since the expectation value of a martingale does not depend on time, by taking the limit $R \rightarrow \infty$ we obtain

$$\mathbf{P}[\gamma \cap A = \emptyset] = \mathbf{P}[\tau_A = \infty] = \Phi'_A(0)^{5/8}. \quad (52)$$

(To make this argument rigorous we would need to show that $M_t^{(5/8)}$ is what is called a local martingale.)

The beautiful Eq. (52) can now be used to show that $\text{SLE}_{8/3}$ satisfies restriction property. To do this, let us consider two different hulls A and B (as in Fig. 5), both a finite distance from the origin, and calculate the conditional probability that the image $\Phi_A(\gamma)$ of an SLE trace does not intersect the hull B , given that the original trace γ does not intersect the hull A . This is done using Eq. (40) for conditional probabilities:

$$\mathbf{P}[\Phi_A(\gamma) \cap B = \emptyset \mid \gamma \cap A = \emptyset] = \frac{\mathbf{P}[\gamma \cap (A \cup \Phi_A^{-1}(B)) = \emptyset]}{\mathbf{P}[\gamma \cap A = \emptyset]}.$$

According to Eq. (52) the denominator is equal to $\Phi'_A(0)^{5/8}$. The hull $A \cup \Phi_A^{-1}(B)$ that appears in the numerator in the last equation is removed by the composition $\Phi_B \circ \Phi_A$ (see Fig. 5), so the probability in the numerator is equal to $(\Phi_B \circ \Phi_A)'(0)^{5/8} = \Phi'_B(\Phi_A(0))^{5/8} \Phi'_A(0)^{5/8} = \Phi'_B(0)^{5/8} \Phi'_A(0)^{5/8}$, where we used the product rule for the derivative and the normalization $\Phi_A(0) = 0$. Combining all this, we get

$$\mathbf{P}[\Phi_A(\gamma) \cap B = \emptyset \mid \gamma \cap A = \emptyset] = \left(\frac{\Phi'_B(0) \Phi'_A(0)}{\Phi'_A(0)} \right)^{5/8} = \Phi'_B(0)^{5/8}.$$

Thus, the image under Φ_A of the subset of the $\text{SLE}_{8/3}$ traces that avoid the hull A has the same distribution as $\text{SLE}_{8/3}$, which, by definition implies restriction property for $\text{SLE}_{8/3}$.

The notion of restriction can be applied to probability measures on sets of random hulls in the upper half plane that are more general than simple curves. These hulls K must be connected, unbounded, and such that $\overline{K} \cap \mathbb{R} = \emptyset$ and $\mathbb{C} \setminus \overline{K}$ is connected. As was proven in Ref. [48], there is a one-parameter family of conformally-invariant measures on such hulls that have the restriction property. For all these measures the probabilities of avoiding a fixed hull A , as before, are given by

$$\mathbf{P}[K \cap A = \emptyset] = \Phi'_A(0)^h, \quad (53)$$

where the restriction exponents $h \geq 5/8$ characterizes a particular probability measure. Restriction measures with exponents $h > 5/8$ are not realized on simple curves. An important example is given by the so called Brownian excursions (two-dimensional Brownian motions conditioned to always stay in the upper half plane) with filled-in holes which satisfy restriction property with $h = 1$.

For any value of κ in the interval $[0, 4]$ other than $8/3$, SLE_κ does not have restriction property, since no value of h makes $M_t^{(h)}$ a martingale, see Eq. (51), and the relation (53) is not satisfied. However, the amount by which SLE_κ fails to satisfy restriction property can be quantified. Namely, let Sf denote the Schwarzian derivative of the function f :

$$Sf(z) = \frac{f'''(z)}{f'(z)} - \frac{3}{2} \left(\frac{f''(z)}{f'(z)} \right)^2.$$

Then

$$\Phi'_t(\xi_t)^h \exp \left(- \frac{c_\kappa}{6} \int_0^t S\Phi_s(\xi_s) ds \right)$$

is a martingale (this is an easy consequence of Itô formula and Eq. (51)), if we choose

$$h = \frac{6 - \kappa}{2\kappa}, \quad c_\kappa = \frac{(8 - 3\kappa)(\kappa - 6)}{2\kappa}. \quad (54)$$

Notice the appearance of the central charge c_κ of the CFT corresponding to SLE_κ . This is quite natural, since distortions of the boundary of the domain in which a CFT is defined cause changes in its partition function, that depend on the central charge. The exponent h in Eq. (54) also has a

meaning in CFT: it is the dimension $h_{1,2}$ of a primary operator that creates a critical curve when inserted on the boundary, see Eq. (96) in Section 8. Restriction property has been used to relate SLE with CFT in Refs. [49, 50, 51, 52, 53].

Finally, let me mention that restriction measures with exponents $h > 5/8$ can be constructed by adding certain Brownian “bubbles” (subsets of 2D Brownian motions that are closed loops) to an SLE curve with $\kappa \leq 4$, see Ref. [48].

7 Calculations with SLE

In this section I will give detailed examples of calculations of various probabilities and geometric characteristics of critical curve using SLE.

7.1 Left passage probability

This section is adapted from Ref. [54].

Let us fix a point $z = x + iy \in \mathbb{H}$ in the upper half of the physical plane. We may ask whether the trace γ passes to the right or to the left of this point. Formally, this is defined using the winding numbers, as follows. We can close the curve $\gamma[0, t]$ by drawing the arc with the radius $|\gamma(t)|$ from the tip of the trace to the point $|\gamma(t)|$ on the positive real axis, and then draw the straight segment in \mathbb{R} to 0. Then the trace γ passes to the left of z if the winding number of the closed curve defined above is 1 for all large times t . Since γ is transient a.s., there is some random time τ such that the winding number is constant for $t \in (\tau, \infty)$. This constant is either 0 or 1, since γ does not cross itself. The random time τ_z for a given z is either ∞ (if $\kappa \leq 4$), or the swallowing time of z . Then the trace γ satisfies

$$\mathbf{P}[\gamma \text{ passes to the left of } z] = \frac{1}{2} + \frac{\Gamma(\frac{4}{\kappa})}{\sqrt{\pi}\Gamma(\frac{4}{\kappa} - \frac{1}{2})} \frac{x}{y} {}_2F_1\left(\frac{1}{2}, \frac{4}{\kappa}; \frac{3}{2}; -\frac{x^2}{y^2}\right).$$

The idea of the proof of this statement, as well as similar statements about crossing probability, is to see what happens in the mathematical plane, and relate events in the mathematical plane with some real-valued random functions of the SLE process. For this purpose we consider the image of z under the shifted function $w_t = w_t(z)$, and define:

$$u_t = \operatorname{Re} w_t, \quad v_t = \operatorname{Im} w_t, \quad q_t = \frac{u_t}{v_t}.$$

Then it is almost obvious, that, γ is to the left of z if and only if $\lim_{t \nearrow \tau_z} q_t = \infty$, and γ is to the right of z if and only if $\lim_{t \nearrow \tau_z} q_t = -\infty$. A heuristic argument for $\kappa \leq 4$ is as follows. In this case the point z is not swallowed ($\tau_z = \infty$). If the trace γ passes to the left of z , then a particle which starts an un-biased isotropic two-dimensional diffusion from z will hit $\mathbb{R} \cup \gamma(0, \infty)$ either in $[0, \infty)$ or from the right side of γ with probability one. By definition (see Section 9 for details), this probability is the harmonic measure of $\gamma(0, \infty) \cup [0, \infty)$ from z . It is conformally invariant, which means that the harmonic measure in the mathematical UHP of $[\xi_t, \infty)$ from $g_t(z)$ tends to 1 as $t \rightarrow \infty$. And this, in turn, means that $\lim_{t \rightarrow \infty} q_t = \infty$.

In the case $4 < \kappa < 8$ the point z is swallowed at some time τ_z which is finite with probability 1. At this time the curve γ closes a loop around z . Then the issue is whether the loop is clockwise or counter-clockwise. In the first case for times t close to τ_z the harmonic measure of $\gamma(0, t) \cup \mathbb{R}$ is mostly concentrated on $[0, \infty)$ and the right side of the curve $\gamma(0, t)$, which implies that $\lim_{t \nearrow \tau_z} q_t = \infty$. For a counter-clockwise loop the same reasoning gives $\lim_{t \nearrow \tau_z} q_t = -\infty$.

Next we will use the Itô formula to write the stochastic equation for q_t , and then the Dynkin formula to find the necessary probability $\mathbf{P}[\lim_{t \rightarrow \infty} q_t = \infty]$. So, first we have equations for u_t and v_t which are just real and imaginary parts of Eq. (15):

$$du_t = \frac{2u_t}{u_t^2 + v_t^2} dt - \sqrt{\kappa} dB_t, \quad dv_t = -\frac{2v_t}{u_t^2 + v_t^2} dt. \quad (55)$$

The two-dimensional variant of the Itô formula now gives (no explicit time dependence)

$$dq_t = \frac{1}{v_t} du_t - \frac{u_t}{v_t^2} dv_t = \frac{4q_t}{u_t^2 + v_t^2} dt - \frac{\sqrt{\kappa}}{v_t} dB_t.$$

This does not look like a standard Itô equation, so we redefine the time variable and the noise. First, the new time \tilde{t} is introduced as

$$\tilde{t}(t) = \int_0^t \frac{dt}{v_t^2}, \quad d\tilde{t} = \frac{dt}{v_t^2}. \quad (56)$$

This is indeed a time change, since $\tilde{t}(t)$ is a monotonously increasing function. Also, notice that as $t \rightarrow \tau_z$, $v_t \rightarrow 0$ sufficiently fast so that $\tilde{t}(\tau_z) = \infty$. In the new time the equation for $q_{\tilde{t}}$ becomes

$$dq_{\tilde{t}} = \frac{4q_{\tilde{t}}}{q_{\tilde{t}}^2 + 1} d\tilde{t} - \frac{\sqrt{\kappa}}{v_t} dB_t.$$

Next we set $d\tilde{B}_t = dB_t/v_t$ and note that $(d\tilde{B}_t)^2 = (dB_t)^2/v_t^2 = dt/v_t^2 = d\tilde{t}$. This means that $B_{\tilde{t}} = \tilde{B}_t$ is the standard Brownian motion with respect to the new time variable \tilde{t} . The equation for $q_{\tilde{t}}$ now has the standard Itô form:

$$dq_{\tilde{t}} = \frac{4q_{\tilde{t}}}{q_{\tilde{t}}^2 + 1} d\tilde{t} - \sqrt{\kappa} dB_{\tilde{t}}. \quad (57)$$

Next we find the diffusion generator for this equation:

$$\hat{A}f(q) = \frac{\kappa}{2} \frac{d^2 f(q)}{dq^2} + \frac{4q}{q^2 + 1} \frac{df(q)}{dq}.$$

If we study this diffusion on an interval (a, b) , where $a < q < b$, then the probability p_b that $q_{\tilde{t}}$ escapes this interval through the right hand point rather than through the left is given by the second of the formulas (32) where $f(q)$ should satisfy the equation

$$\frac{\kappa}{2} f''(q) + \frac{4q}{q^2 + 1} f'(q) = 0. \quad (58)$$

This equation has a constant solution, but this solution is not what we need, obviously. The other solution is found by straightforward separation of variables (and some specific choice of the constants of integration):

$$f(q) = \int_0^q \frac{dr}{(r^2 + 1)^{4/\kappa}}. \quad (59)$$

We expand the integrand in powers of r and integrate term by term:

$$f(q) = \int_0^q dr \sum_{m=0}^{\infty} (4/\kappa)_m \frac{(-r^2)^m}{m!} = q \sum_{m=0}^{\infty} \frac{(4/\kappa)_m (-q^2)^m}{2m+1 m!}.$$

Here $(a)_m$ denotes the Pochhammer symbol $(a)_m = \Gamma(a+m)/\Gamma(a)$. Using this notation we can write

$$\frac{1}{m+a} = \frac{\Gamma(m+a)}{\Gamma(m+1+a)} = \frac{\Gamma(a)}{\Gamma(1+a)} \frac{(a)_m}{(1+a)_m} = \frac{1}{a} \frac{(a)_m}{(1+a)_m}, \quad (60)$$

and, in particular, $1/(2m+1) = (1/2)_m/(3/2)_m$. This gives

$$f(q) = q \sum_{m=0}^{\infty} \frac{(1/2)_m (4/\kappa)_m (-q^2)^m}{(3/2)_m m!} = q {}_2F_1\left(\frac{1}{2}, \frac{4}{\kappa}; \frac{3}{2}; -q^2\right).$$

Using asymptotics of the hypergeometric function we see that the solution $f(q)$ has finite limits

$$\lim_{q \rightarrow \pm\infty} f(q) = \pm \frac{\sqrt{\pi} \Gamma(\frac{4}{\kappa} - \frac{1}{2})}{2 \Gamma(\frac{4}{\kappa})}.$$

This shows that the considered diffusion of $q_{\tilde{t}}$ is transient, meaning that with a finite probability $\lim_{\tilde{t} \rightarrow \infty} q_{\tilde{t}} = \infty$. Thus, we can finally take limits $a \rightarrow -\infty, b \rightarrow \infty$ and get the result

$$\begin{aligned} \mathbf{P}[\gamma \text{ passes to the left of } z] &= \mathbf{P}[\lim_{t \nearrow \tau_z} q_t = \infty] \\ &= \frac{f(x/y) - f(-\infty)}{f(\infty) - f(-\infty)} = \frac{1}{2} + \frac{\Gamma(\frac{4}{\kappa})}{\sqrt{\pi} \Gamma(\frac{4}{\kappa} - \frac{1}{2})} \frac{x}{y} {}_2F_1\left(\frac{1}{2}, \frac{4}{\kappa}; \frac{3}{2}; -\frac{x^2}{y^2}\right). \end{aligned}$$

When $\kappa = 2, 8/3, 4$ and 8 , the last formula simplifies to

$$1 + \frac{xy}{\pi|z|^2} - \frac{\arg z}{\pi}, \quad \frac{1}{2} + \frac{x}{2|z|}, \quad 1 - \frac{\arg z}{\pi}, \quad \frac{1}{2},$$

respectively.

The value $1/2$ obtained for $\kappa = 8$ is somewhat misleading. The point is that if $\kappa \geq 8$, then the curve γ densely fills the upper half plane, as was mentioned in Section 6.2, and goes *through* every point, not to the left or right of it. This is reflected in the fact that for $\kappa \geq 8$ the function $f(q)$ in Eq. (59) diverges as $q \rightarrow \pm\infty$. This divergence means that to determine the fate of the process $q_{\tilde{t}}$ as $\tilde{t} \rightarrow \infty$, we need to start with a finite interval (a, b) ($a < x/y < b$) and take the limits $a \rightarrow -\infty$ and $b \rightarrow \infty$ separately. In both cases we find that $\mathbf{P}[\lim_{t \nearrow \tau_z} q_t = \pm\infty] = 0$, meaning that $q_{\tilde{t}}$ always stays bounded. See a related discussion in Section 7.3.

7.2 Cardy's formula for crossing probability

The problem is first posed in a rectangle ABCD. We need to find the probability that there is a percolation cluster connecting the left side AB and the right side CD of the rectangle, where we impose the fixed boundary condition ($p = 1$). Note that from the point of view suggested by SLE, we need to consider not the cluster itself, but one of its "boundaries", upper or lower. Let us consider the lower boundary, which in the continuous limit is described by SLE_6 . Then we see that if there is a spanning cluster, then the boundary will necessarily start at the point B, and will reach the side CD

without touching the upper side AD. In the opposite case, when there is no spanning cluster, the boundary will touch AD before touching CD.

In fact, this reformulation of the problem can be generalized to any $\kappa > 4$, and we will assume this has been done.

Next we conformally map the rectangle to the upper half plane using the Schwarz-Christoffel formula. The direct mapping $\Phi(z)$ (from rectangle to the UHP) is given by an elliptic function, and the inverse mapping—by an elliptic integral. Postponing the details until the end of this section, let us assume for now that the images of the vertices of the rectangle are

$$\Phi(A) = a < 0, \quad \Phi(B) = 0, \quad \Phi(C) = c > 0, \quad \Phi(D) = \infty. \quad (61)$$

Since the crossing probability is conformally invariant (as a property of SLE), we are now interested in the following question. Since $\kappa > 4$, both points a and c will be swallowed at some finite random times τ_a and τ_c . The crossing probability then is $\mathbf{P}[\tau_c < \tau_a]$, that is, the probability that the point c is swallowed before the point a .

As should be obvious by now, we need to study the motion of the images of the points a, b under the Loewner map. In this case it is easier to use the original map (before the shift), so we define

$$a_t = g_t(a), \quad c_t = g_t(c), \quad r_t = \frac{\xi_t - a_t}{c_t - a_t}.$$

The variable r_t is normalized to lie between 0 and 1, and we are essentially interested in the probability $\mathbf{P}[c_\tau = \xi(\tau)] = \mathbf{P}[r_\tau = 1]$, where τ is the escape time from $[0, 1]$ for r_t .

The calculations are straightforward:

$$d(\xi - a_t) = d\xi - \frac{2}{a_t - \xi} dt, \quad d(c_t - a_t) = \left(\frac{2}{c_t - \xi} - \frac{2}{a_t - \xi} \right) dt.$$

Then

$$\begin{aligned} dr_t &= \frac{d(\xi - a_t)}{c_t - a_t} - \frac{\xi - a_t}{(c_t - a_t)^2} d(c_t - a_t) \\ &= \left(\frac{1}{r_t} - \frac{1}{1 - r_t} \right) \frac{2dt}{(c_t - a_t)^2} + \frac{\sqrt{\kappa}}{c_t - a_t} dB_t. \end{aligned}$$

Again, this SDE is not of the Itô type, and we perform a time change:

$$d\tilde{t} = dt / (c_t - a_t)^2, \quad d\tilde{B}_t = dB_t / (c_t - a_t).$$

Then the process $\tilde{r}_t = r_{\tilde{t}}$ satisfies the Itô equation

$$dr_{\tilde{t}} = 2\left(\frac{1}{r_{\tilde{t}}} - \frac{1}{1-r_{\tilde{t}}}\right)d\tilde{t} + \sqrt{\kappa}dB_{\tilde{t}}.$$

The generator of diffusion for this process is

$$\hat{A} = \frac{\kappa}{2} \frac{d^2}{dr^2} + 2\left(\frac{1}{r} - \frac{1}{1-r}\right) \frac{d}{dr},$$

and its zero mode $f(r)$ is found by simple integrations as before:

$$f(r) = \int_0^r \frac{ds}{(s(1-s))^{4/\kappa}}.$$

Since $\kappa > 4$, the last integral converges both at the lower and the upper limits, when $r \rightarrow 1$. As in the previous section, using Eq. (60) this integral can be expressed in terms of the Gauss hypergeometric function:

$$\begin{aligned} f(r) &= \int_0^r ds s^{-4/\kappa} \sum_{m=0}^{\infty} (4/\kappa)_m \frac{s^m}{m!} = r^{1-4/\kappa} \sum_{m=0}^{\infty} \frac{(4/\kappa)_m}{m+1-\frac{4}{\kappa}} \frac{r^m}{m!} \\ &= \frac{1}{1-\frac{4}{\kappa}} r^{1-4/\kappa} \sum_{m=0}^{\infty} \frac{(4/\kappa)_m (1-4/\kappa)_m}{(2-4/\kappa)_m} \frac{r^m}{m!} \\ &= \frac{1}{1-\frac{4}{\kappa}} r^{1-4/\kappa} {}_2F_1\left(\frac{4}{\kappa}, 1-\frac{4}{\kappa}; 2-\frac{4}{\kappa}; r\right). \end{aligned}$$

At the ends of the interval for diffusion of r_t this function takes the values $f(0) = 0$ and $f(1) = \Gamma^2(1-4/\kappa)/\Gamma(2-8/\kappa)$. Substituting this into Eq. (32) with $a = 0, b = 1$, we get the final result

$$\mathbf{P}[\text{crossing}] = \frac{\Gamma(2-\frac{8}{\kappa})}{\Gamma(2-\frac{4}{\kappa})\Gamma(1-\frac{4}{\kappa})} r^{1-4/\kappa} {}_2F_1\left(\frac{4}{\kappa}, 1-\frac{4}{\kappa}; 2-\frac{4}{\kappa}; r\right). \quad (62)$$

As usual, here r means the initial value of the process r_t , that is, $r = -a/(c-a)$. For $\kappa = 6$ this reduces to Cardy's formula for crossing probability for percolation [55].

Now we can discuss how to map a given rectangle to the UHP. Suppose the horizontal and vertical sides of the rectangle have lengths L and L' . It is obvious that the crossing probability is invariant under rescaling. Then we need to find the (unique) number $0 < k < 1$ (the so called elliptic modulus) from the equation

$$\frac{L'}{L} = \frac{K'(k)}{2K(k)},$$

where $K(k)$ is the complete elliptic integral of the first kind, and $K'(k) = K(\sqrt{1-k^2})$ (in the following we simplify these to K, K'). Next we rescale the rectangle and place its vertices as follows:

$$A = -K + iK', \quad B = -K, \quad C = K, \quad D = K + iK'.$$

It is easy to see then that the function

$$\Phi(z) = k \frac{1 + \operatorname{sn}(z, k)}{1 - k \operatorname{sn}(z, k)}$$

maps the interior of our rectangle to the UHP, and its vertices to

$$\Phi(A) = -\frac{1-k}{2}, \quad \Phi(B) = 0, \quad \Phi(C) = \frac{2k}{1-k}, \quad \Phi(D) = \infty.$$

Comparing this with Eq. (61) we obtain $r = \left(\frac{1-k}{1+k}\right)^2$, which we need to substitute to Eq. (62) to get the crossing probability for the rectangle.

7.3 Fractal dimensions of SLE curves

SLE curves are fractal objects. Their fractal dimension can be estimated by the box counting dimension. Namely, we can ask how the number of small disks of radius ϵ required to cover an $\operatorname{SLE}_\kappa$ curve scales with ϵ :

$$N_\epsilon \sim \epsilon^{-d_f(\kappa)},$$

where $d_f(\kappa)$ is the box counting fractal dimension. Strictly speaking, this definition is applicable only for finite curves, but it can be applied for any segment of a chordal SLE curve, since all the segments should be statistically similar.

The fractal dimension $d_f(\kappa)$ is related to multifractal exponents of the harmonic measure, and can be obtained from them, as explained in Section 9. In this section we use a probabilistic approach.

The dimension $d_f(\kappa)$ can be estimated in the spirit of Monte-Carlo methods by throwing disks of radius ϵ randomly onto the domain containing the critical curve, and then counting the fraction of the disks which intersect the curve. Alternatively, we can look for the probability that an SLE curve intersects a *given* disk. It is clear that this probability should scale as $\epsilon^{2-d_f(\kappa)}$ (2 here is the dimensionality of the physical plane), and it is this scaling

that can be relatively easily obtained from SLE, with the result (rigorously established in Refs. [36, 37], see also an earlier discussion in Ref. [35])

$$d_f(\kappa) = \min\left(1 + \frac{\kappa}{8}, 2\right). \quad (63)$$

To derive this scaling we need to introduce some notation and properties of conformal maps. First, let D be a domain in the complex plane, ∂D its boundary, and z a point inside D . Denote by $\text{dist}(z, \partial D)$ the Euclidean distance between z and the domain boundary.

If the domain D is mapped conformally to a domain \tilde{D} by a function $\tilde{z} = f(z)$, then the distance between close points z and $z + dz$ gets multiplied by a rescaling factor: $|d\tilde{z}| = |f'(z)||dz|$. The same is roughly speaking true for finite distances. More precisely, if $d = \text{dist}(z, \partial D)$ and $\tilde{d} = \text{dist}(\tilde{z}, \partial \tilde{D})$, then a corollary to the famous Koebe 1/4 theorem states that

$$\frac{\tilde{d}}{4d} \leq |f'(z)| \leq \frac{4\tilde{d}}{d} \quad \text{or} \quad \frac{\tilde{d}}{4|f'(z)|} \leq d \leq \frac{4\tilde{d}}{|f'(z)|}. \quad (64)$$

Let us denote these bounds by $d \asymp \tilde{d}/|f'(z)|$ and say that both quantities are comparable.

Now we apply this to the Loewner map $w_t(z)$ to estimate the limit of the distance $d_t(z) = \text{dist}(z, \gamma(0, t) \cup \mathbb{R})$ between a point z and an SLE curve in the physical plane, as the time goes up to the swallowing time τ_z (which may be infinite). We use the same notation as in section 7.1, and write $w_t(z) = w_t = u_t + iv_t$ for the image of the point z . In the mathematical plane the distance from the image to the boundary is simply $\text{Im } w_t(z) = v_t$. If we introduce the process

$$D_t(z) = \log \frac{|w'_t(z)|}{\text{Im } w_t(z)},$$

Eq. (64) gives $d_t(z) \asymp e^{-D_t(z)}$. Let us find the SDE for $D_t(z)$. First, the z -derivative of the basic SLE equation (15) gives

$$\partial_t \log w'_t(z) = -\frac{2}{w_t^2(z)}.$$

The real part of this equation is

$$\partial_t \log |w'_t(z)| = -\frac{2 \text{Re}[w_t^2(z)]^*}{|w_t(z)|^4} = 2 \frac{v_t^2 - u_t^2}{(v_t^2 + u_t^2)^2}. \quad (65)$$

Combining this with the Eq. (55) for v_t , we get

$$\partial_t D_t(z) = \frac{4v_t^2}{(v_t^2 + u_t^2)^2} \geq 0.$$

Thus, $D_t(z)$ increases with t , and to estimate $d(z) = \text{dist}(z, \gamma(0, \infty) \cup \mathbb{R}) \asymp e^{-D(z)}$ we need to look at

$$D(z) = \lim_{t \nearrow \tau_z} D_t(z) = \int_0^{\tau_z} \frac{4v_t^2}{(v_t^2 + u_t^2)^2} dt.$$

As in Section 7.1 we change time according to (56) and get

$$D(x/y) = 4 \int_0^\infty \frac{d\tilde{t}}{(q_{\tilde{t}}^2 + 1)^2}, \quad (66)$$

where the process $q_{\tilde{t}} = u_{\tilde{t}}/v_{\tilde{t}}$ satisfies the SDE (57) and has the initial value x/y . As we discussed in the end of Section 7.1, if $\kappa \geq 8$ the process $q_{\tilde{t}}$ stays bounded as $\tilde{t} \rightarrow \infty$. Then the integral in Eq. (66) diverges, and $D(x/y) = \infty$. This immediately gives that $d(z) = 0$ and

$$d_f(\kappa \geq 8) = 2, \quad (67)$$

consistent with the curve γ densely filling the upper half plane.

Now consider the case $0 \leq \kappa < 8$. Since $d(z) \asymp e^{-D(x/y)}$, the probability $\mathbf{P}[\Delta(z) \leq \epsilon]$ that the SLE curve intersects the disc of radius ϵ centered at the point z is comparable to (scales in the same way with ϵ as) the probability $\mathbf{P}[D(x/y) \geq -\log \epsilon]$. The latter probability can be estimated if we find the asymptotics of the probability distribution function $p(D, x/y)$ for $D(x/y)$.

We expect that the scaling of $\mathbf{P}[d(z) \leq \epsilon]$ with ϵ should not depend on the actual position of z . In fact, the SLE scaling property (41) implies that $d(x+iy)$ has the same distribution as $yd(\frac{x}{y}+i)$, and thus we are free to choose the point z anywhere. To simplify the formulas below, we will now take the point z to be $x+i$. Then the process $q_{\tilde{t}}$ starts at $q_0 = x$ and is transient, that is, goes to ∞ or $-\infty$. In both cases the integral (66) is convergent and non-negative, and we can use the stationary FK formulas (37, 38) from Section 5.5 to find $p(D, x)$ through its Laplace transform $L(s, x)$. Namely, $L(s, x)$ should satisfy

$$\frac{\kappa}{2} \frac{d^2 L}{dx^2} + \frac{4x}{x^2 + 1} \frac{dL}{dx} - \frac{4s}{(x^2 + 1)^2} L = 0.$$

The change of variables $y = x^2/(x^2 + 1)$ leads to the hypergeometric equation

$$y(1-y)\frac{d^2L}{dy^2} + \left[\frac{1}{2} + \left(\frac{4}{\kappa} - 2\right)y\right]\frac{dL}{dy} - \frac{2s}{\kappa}L = 0.$$

The solution of this equation normalized as $L(s, x = \infty) = 1$ is

$$L(s, x) = \frac{\Gamma(\frac{1}{2} - a_+)\Gamma(\frac{1}{2} - a_-)}{\Gamma(\frac{1}{2})\Gamma(\frac{4}{\kappa} - \frac{1}{2})} {}_2F_1\left(a_+, a_-; \frac{1}{2}; \frac{x^2}{x^2 + 1}\right), \quad (68)$$

$$a_{\pm}(s) = \frac{1}{2} - \frac{2}{\kappa} \pm \sqrt{\left(\frac{1}{2} - \frac{2}{\kappa}\right)^2 - \frac{2s}{\kappa}}.$$

The inverse Laplace transform give the probability density for D :

$$p(D, x) = \frac{1}{2\pi i} \int_{c-i\infty}^{c+i\infty} e^{sD(x)} L(s, x) ds.$$

The integration contour should lie to the right of all the singularities of $L(s, x)$ in the s -plane. If we deform the contour by moving it to the left, it will encircle the poles of $L(s, x)$, and for large $D(x)$ the leading behavior of $p(D, x)$ will be determined by the pole with the largest real part.

Let us now find the singularities of $L(s, x)$ given by Eq. (68). Since the hypergeometric function ${}_2F_1(a, b; c; x)$ is an entire function of its parameters a, b, c , the only singularities of $L(s, x)$ are in the prefactor in Eq. (68). Gamma functions have poles when their arguments are non-positive integers: $1/2 - a_{\pm}(s) = -n$, $n \geq 0$, which gives the poles at real positions

$$s_n = -1 + \frac{\kappa}{8} - 2n - \frac{\kappa}{2}n^2.$$

The largest pole is at $s_0 = -1 + \kappa/8$, which gives for large D

$$p(D, x) \propto e^{-(1-\kappa/8)D}.$$

Finally, we have the estimate

$$\mathbf{P}[d(x+i) \leq \epsilon] \asymp \mathbf{P}[D(x) \geq -\log \epsilon] = \int_{-\log \epsilon}^{\infty} p(D, x) dD \propto \epsilon^{1-\kappa/8},$$

which gives

$$d_f(\kappa < 8) = 1 + \frac{\kappa}{8}. \quad (69)$$

Together with (67) this establishes Eq. (63).

7.4 Derivative expectation

The absolute value of the derivative of the SLE map $|w'_t(z)|$ and its moments are useful quantities. As for any conformal map $|w'_t(z)|$ is the local measure of rescaling introduced by the map. For a critical curve described by SLE the moments $\mathbf{E}[|w'_t(z)|^h]$ where $h \in \mathbb{R}$, are also related to the spectrum of multifractal exponents of the harmonic measure, as explained in Section 9. In this context the derivative should be estimated at a certain distance from an SLE curve. Alternatively, of all the SLE curves we should choose only the ones that pass closer than a certain small distance ϵ from a given point z . This is an example of conditioning introduced in Section 5.6.

Finding the conditional expectation value $\mathbf{E}[|w'_t(z)|^h; d(z) \leq \epsilon]$ at point z in the bulk is a difficult problem that has not been solved so far (see, however, how similar quantities are calculated in Refs. [11, 35]). However, each SLE curve starts at the origin in the physical plane, and no conditioning is required to estimate the derivative of the SLE map at real point x on the boundary.

Indeed, in this case Eq. (65) simplifies (since $v_t = 0$) and gives in the notation of Section 6.2.1

$$\partial_t \log |w'_t(x)| = -\frac{2}{x_t^2}, \quad |w'_t(x)|^h = \exp\left(-2h \int_0^t \frac{ds}{x_s^2}\right). \quad (70)$$

According to the Feynman-Kac formula (34) the expectation value $c(x, t) = \mathbf{E}[|w'_t(x)|^h]$ satisfies

$$\partial_t c(x, t) = \frac{\kappa}{2} \partial_x^2 c(x, t) + \frac{2}{x} \partial_x c(x, t) - \frac{2h}{x^2} c(x, t), \quad c(x, 0) = 1.$$

From the SLE scaling law (5) we know that x and t must appear in the combination x/\sqrt{t} . With some hindsight we denote $y = x^2/2\kappa t$ and $c(x, t) = f(y)$. Then the equation and the boundary value for $f(y)$ become

$$y^2 f''(y) + y\left(\frac{2}{\kappa} + \frac{1}{2} + y\right) f'(y) - \frac{h}{\kappa} f(y) = 0, \quad \lim_{y \rightarrow \infty} f(y) = 1.$$

In the limit $y \rightarrow 0$ (long times) we can neglect y in the brackets in front of f' , and the equation simplifies to an Euler equation with the solution $y^{\Delta(h)/2}$, where

$$\Delta(h) = \frac{\kappa - 4 + \sqrt{(\kappa - 4)^2 + 16\kappa h}}{2\kappa} \quad (71)$$

is a solution of the indicial equation that vanishes as $h \rightarrow 0$.

In the context of the problem of multifractal exponents of harmonic measure the scaling

$$\mathbf{E}[|w'_t(x)|^h] \sim \left(\frac{|x|}{\sqrt{2\kappa t}}\right)^{\Delta(h)}$$

is all we need. But we can also solve the problem completely. Namely, if we write $f(y) = e^{-y}y^{\Delta(h)/2}\psi(y)$, then $\psi(y)$ satisfies

$$y\psi''(y) + (c - y)\psi'(y) - a\psi(y) = 0, \quad \psi(y \rightarrow \infty) \rightarrow e^y y^{-\Delta(h)/2},$$

$$a = \frac{2}{\kappa} + \frac{1}{2} + \frac{\Delta(h)}{2}, \quad c = \frac{2}{\kappa} + \frac{1}{2} + \Delta(h),$$

which is the standard form of the differential equation for the confluent hypergeometric function. The solution with the required asymptotic behavior is $[\Gamma(a)/\Gamma(c)]\Phi(a, c; y)$, and we finally get

$$\mathbf{E}[|w'_t(x)|^h] = \frac{\Gamma(a)}{\Gamma(c)} \left(\frac{|x|}{\sqrt{2\kappa t}}\right)^{\Delta(h)} e^{-x^2/2\kappa t} \Phi\left(a, c; \frac{x^2}{2\kappa t}\right).$$

8 Critical curves and bosonic fields (Coulomb gas)

In the rest of this review I will provide a connection between SLE and a more traditional approach to critical 2D systems, namely, conformal field theory (CFT). In this Section we will see how critical curves can be described within a CFT of a scalar field. Closely related discussions have appeared before in Refs. [56, 57, 58].

8.1 From loop models to bosonic fields

The relation between critical curves and operators of a boundary CFT is most transparent in their representation by a Gaussian boson field $\varphi(z, \bar{z})$ [19, 22, 59, 60]. This representation is commonly known as the Coulomb gas method. Specifically, let us consider the $O(n)$ model on a honeycomb lattice. In the hope of describing the critical point by a local field theory, we need to have a description in terms of local weights on the lattice.

To reproduce the partition function (1) we randomly assign orientations to loops and then sum over all possible arrangements. The sum of weights for two orientations of every loop should give n . This is achieved by giving the local weight $e^{\pm ie_0\pi/6}$ to each lattice site where an oriented loop makes right (left) turn. The weight of an oriented closed loop is the product of

all local site weights, and is equal to $e^{\pm ie_0\pi}$ since for a closed loop the difference between the numbers of right and left turns is ± 6 . The sum over the orientations reproduces the correct weight n for an un-oriented loop if we choose

$$n = 2 \cos \pi e_0.$$

The range of $-2 \leq n \leq 2$ where the loops of $O(n)$ are critical can be covered once by $e_0 \in [0, 1]$. However, as we will see, to describe both the dilute and the dense phases we need to allow for a wider range $e_0 \in [-1, 1]$, with positive e_0 for the dense phase and negative e_0 for the dilute phase.

For each configuration of oriented loops we can define a real height variable H that resides on the dual lattice and takes discrete values conventionally chosen to be multiples of π . To define H we start at some reference point where we set $H = 0$, and then every time we cross an oriented loop, we change H by $\pm\pi$ depending on whether we cross the loop from its left to its right side or vice versa. Since the orientation of the loops was introduced randomly, the height function has to be compactified with radius $\mathcal{R} = 1$:

$$H \simeq H + 2\pi, \tag{72}$$

which means that the heights H and $H + 2\pi$ correspond to the same configuration of un-oriented loops.

At criticality, the coarse-grained height function becomes a continuous scalar field (boson), believed to be described by the Gaussian action $(g/4\pi) \int_D d^2x (\nabla H)^2$, where the fluctuation strength parameter g is not yet determined. This can be done either by comparison with exact solutions of a related six-vertex model, or by an elegant argument due to Kondev and Henley [61, 62] (which, unfortunately, only works in the dense phase). Here's the argument.

If the system is defined on a domain with boundaries, some loops may not be counted with the correct statistical weight. For example, the difference between the numbers of left and right turns for a loop that wraps around a cylinder is 0 rather than 6. Therefore, without modifications all such loops will be counted with a wrong weight 2 in the partition function. This is fixed by adding to the action a boundary term $(ie_0/2\pi) \int_{\partial D} dl KH$, where K is the geodesic curvature of the boundary. Each loop wrapped around the cylinder introduces an additional height difference $\Delta H = \pm\pi$ between the ends thus acquiring the correct weight.

A similar situation occurs if the critical system lives on a surface with curvature, which microscopically can be viewed as existence of defects on

the honeycomb lattice (pentagons and heptagons correspond to positive and negative curvature, correspondingly). The correct weight for a loop that surrounds a region of non-zero curvature is obtained only if we include in the action the so-called background charge term $(ie_0/8\pi) \int_D d^2x RH$, where R is the scalar curvature.

Yet another necessary term in the action is the *locking potential* of the form $\lambda \int d^2x V(H)$ which would force the discrete values $H = k\pi$ in the limit $\lambda \rightarrow \infty$. It must be, therefore, a π -periodic function of H , the most general form of it being $V = \sum_{k \in \mathbb{Z}, k \neq 0} v_k e^{2ikH}$. Each term of V is a vertex operator whose dimension is [22]

$$x_k = \frac{2}{g} k(k - e_0).$$

Most of these terms are irrelevant at the Gaussian fixed point, and we can ignore them. The most relevant term has $k = 1$ if $0 < e_0 < 1$, and it has to be strictly marginal ($x_k = 2$) in order to retain the conformal invariance of the action. This gives the relations

$$e_0 = 1 - g, \quad n = -2 \cos \pi g. \quad (73)$$

In this case $0 < g < 1$, which is known to describe the dense phase of the $O(n)$ model. In the dilute phase the second relation (73) still holds [22], but with $1 \leq g \leq 2$. This range is not possible to obtain from the previous argument since for $-1 < e_0 < 0$ we would need to pick $k = -1$ term as the most relevant, and it would still give us $g = 1 + e_0 = 1 - |e_0| < 1$. With some amount of hindsight we will assume *both* relations (73) to be valid for the whole range $g \in (0, 2]$ encompassing both the dense and the dilute phase. The point $g = 1$ separating the phases is somewhat special: there we need to keep both $k = 1$ and $k = -1$ terms in the locking potential since they have the same dimension.

The failure of Kondev's argument in the dilute phase has a very significant geometric meaning. Namely, upon the coarse-graining the $O(n)$ loops become level lines of the bosonic field. However this identification can only be made for the dense phase, where the loops come close to themselves and each other on the lattice, translating to them becoming non-simple curves (with double points) in the continuum limit, resembling the traces of SLE with $\kappa > 4$. The relation between critical lines and the bosonic field is quite different in the dilute phase, and this difference is related to quite a few subtleties in the treatment of both the dilute and the dense phases of a *bounded* system in the Coulomb gas formalism. For details see our paper [21].

We now introduce the parametrization

$$g = \frac{4}{\kappa}, \quad 2 \leq \kappa < \infty, \quad (74)$$

where κ can be identified with the SLE parameter by comparing calculations of some quantity within the two approaches. A typical example is the distribution of winding angles of critical curves on a cylinder, which is known through both the Coulomb gas method and SLE. Another good example is the multifractal exponents related to derivative expectations, which we compute in the Coulomb gas formalism in Section 9. Notice that $\kappa < 4$ and $\kappa > 4$ describe the dilute and the dense phases, correspondingly, while $\kappa = 4$ gives the point $g = 1$ separating the two phases. All this is quite consistent with the SLE phases determined in Section 6.2.

In the CFT literature it is customary to rescale the field $\varphi = \sqrt{2g}H$ and make the coupling constant fixed $g_{\text{new}} = 1/2$, at the expense of varying the compactification radius of φ :

$$\mathcal{R} = \sqrt{8/\kappa}. \quad (75)$$

This is the normalization that we adopt from now on. For the rescaled field the action with all the terms becomes

$$\begin{aligned} S[\varphi] = & \frac{1}{8\pi} \int_D d^2x [(\nabla\varphi)^2 + i2\sqrt{2}\alpha_0 R\varphi] + i\frac{\sqrt{2}\alpha_0}{2\pi} \int_{\partial D} dl K\varphi \\ & + \int_D d^2x e^{i\sqrt{2}\alpha_+\varphi}, \end{aligned} \quad (76)$$

where we use the notation

$$\begin{aligned} 2\alpha_0 = \frac{\sqrt{\kappa}}{2} - \frac{2}{\sqrt{\kappa}}, & \quad \alpha_{\pm} = \alpha_0 \pm \sqrt{\alpha_0^2 + 1}, \\ \alpha_+ = \sqrt{\kappa}/2, & \quad \alpha_- = -2/\sqrt{\kappa}. \end{aligned} \quad (77)$$

Notice that α_0 is proportional to e_0 , and can be both positive and negative, its sign being different in the two phases of the loop model.

8.2 Coulomb gas CFT in the bulk

Consider now our bosonic theory on the infinite plane (the Riemann sphere), dropping for now the boundary term in Eq. (76). The action $S[\varphi]$ does not describe a free field because of the presence of the locking potential. In

practice, however, this potential is always treated perturbatively, and any correlation function is expanded as

$$\langle X \rangle_S = \sum_{n=0}^{\infty} \frac{1}{n!} \int d^2x_1 \dots \int d^2x_n \langle e^{i\sqrt{2}\alpha_+\varphi(x_1)} \dots e^{i\sqrt{2}\alpha_+\varphi(x_n)} X \rangle, \quad (78)$$

where $\langle \dots \rangle$ stands for correlators in the free theory with action

$$S_0 = \frac{1}{8\pi} \int_D d^2x [(\nabla\varphi)^2 + i2\sqrt{2}\alpha_0 R\varphi]. \quad (79)$$

The neutrality condition discussed below makes sure that for a given operator X , at most one term survives in the sum in Eq. (78). The free action S_0 is known to describe a CFT with the central charge

$$c_\kappa = 1 - 24\alpha_0^2 = 1 - 3\frac{(\kappa - 4)^2}{2\kappa}, \quad (80)$$

which is the same as Eq. (18). The holomorphic part of the stress-energy tensor corresponding to the central charge (80) is

$$T = -\frac{1}{2} :(\partial\varphi)^2: + i\sqrt{2}\alpha_0 \partial^2\varphi, \quad (81)$$

where $\partial = \partial/\partial z$, and semicolons stand for normal ordering.

Notice that by the appropriate choice of metric, the curvature R may be made to vanish everywhere in the finite region of the plane. The curvature is then concentrated at infinity, and its effect is represented by insertion of a certain vertex operator ($V_{-2\alpha_0, -2\alpha_0}$ in the notation of Eq. (84) below) in the correlation functions, thereby changing the neutrality condition, see discussion below. This prescription, due to Dotsenko and Fateev [23], allows to calculate correlators of primary fields (vertex operators) using simple free boson with $c = 1$ described by the action (79) but with $\alpha_0 = 0$:

$$S_0 = \frac{1}{8\pi} \int_D d^2x (\nabla\varphi)^2. \quad (82)$$

In the complex coordinates $z = x + iy$, $\bar{z} = x - iy$ the field φ separates into the holomorphic and antiholomorphic parts:

$$\varphi(z, \bar{z}) = \phi(z) + \bar{\phi}(\bar{z}),$$

and the basic correlators of these fields follow from (82):

$$\langle \phi(z)\phi(z') \rangle = -\log(z - z'), \quad \langle \bar{\phi}(\bar{z})\bar{\phi}(\bar{z}') \rangle = -\log(\bar{z} - \bar{z}'), \quad \langle \phi(z)\bar{\phi}(\bar{z}) \rangle = 0. \quad (83)$$

Primary fields in the theory (79) are electric (vertex) and magnetic (vortex) operators, and their combinations also called vertex operators for simplicity (they all are implicitly assumed to be normal ordered):

$$\begin{aligned} V_{e,0}(z, \bar{z}) &= e^{i\sqrt{2}e\varphi(z, \bar{z})}, & V_{0,m}(z, \bar{z}) &= e^{-\sqrt{2}m\tilde{\varphi}(z, \bar{z})}, \\ V_{e,m}(z, \bar{z}) &= e^{i\sqrt{2}e\varphi(z, \bar{z})}e^{-\sqrt{2}m\tilde{\varphi}(z, \bar{z})}, \end{aligned}$$

where we introduced the Cauchy-Riemann dual

$$\tilde{\varphi}(z, \bar{z}) = -i\phi(z) + i\bar{\phi}(\bar{z})$$

of the field φ , as well as electric and magnetic charges e and m . A general vertex operator can also be written as a product of holomorphic and antiholomorphic components:

$$\begin{aligned} V_\alpha(z) &= e^{i\sqrt{2}\alpha\phi(z)}, & \bar{V}_{\bar{\alpha}}(\bar{z}) &= e^{i\sqrt{2}\bar{\alpha}\bar{\phi}(\bar{z})}, \\ V_{\alpha, \bar{\alpha}}(z, \bar{z}) &= V_\alpha(z)\bar{V}_{\bar{\alpha}}(\bar{z}) = e^{i\sqrt{2}\alpha\phi(z)}e^{i\sqrt{2}\bar{\alpha}\bar{\phi}(\bar{z})}, \end{aligned} \quad (84)$$

where the holomorphic and antiholomorphic charges are:

$$\alpha = e + m, \quad \bar{\alpha} = e - m.$$

The holomorphic and antiholomorphic dimensions of the vertex operators follow from the anomalous stress-energy tensor (81):

$$\begin{aligned} h(\alpha) &= \alpha(\alpha - 2\alpha_0) = h(e, m) = (e + m)(e + m - 2\alpha_0), \\ \bar{h}(\bar{\alpha}) &= \bar{\alpha}(\bar{\alpha} - 2\alpha_0) = \bar{h}(e, m) = (e - m)(e - m - 2\alpha_0). \end{aligned}$$

From this we see that a vertex operator is spinless (meaning that $h = \bar{h}$) if either $\bar{\alpha} = \alpha$ or $\bar{\alpha} = 2\alpha_0 - \alpha$. In the first case the operator is purely electric ($m = 0$), and in the second case it can have an arbitrary magnetic charge, but the electric charge should be $e = \alpha_0$. We then introduce the notation

$$V^{(\alpha)}(z, \bar{z}) = V_\alpha(z)\bar{V}_{2\alpha_0 - \alpha}(\bar{z}). \quad (85)$$

Notice also a certain duality: the dimensions of the operators V_α and $V_{2\alpha_0 - \alpha}$ are the same. This is consistent with the correlator

$$\langle V_\alpha(z)V_{2\alpha_0 - \alpha}(z') \rangle = (z - z')^{-2h_\alpha}.$$

We see that the sum of the charges of the operators within the correlator is $2\alpha_0$, which is the negative of the background charge $-2\alpha_0$ placed at infinity.

This is true in general: in the theory with a background charge correlators of vertex operators do not vanish only if the following neutrality condition is satisfied — the total sum of charges should equal to $2\alpha_0$, in which case the chiral correlator is given by

$$\langle V_{\alpha_1}(z_1)V_{\alpha_2}(z_2)\dots V_{\alpha_n}(z_n)\rangle = \prod_{i<j}(z_i - z_j)^{2\alpha_i\alpha_j}, \quad \sum_i \alpha_i = 2\alpha_0. \quad (86)$$

Similarly, the correlator of vertex operators $V_{\alpha,\alpha}(z, \bar{z})$ is

$$\langle \prod_i V_{\alpha_i,\alpha_i}(z_i, \bar{z}_i)\rangle = \prod_{i<j} |z_i - z_j|^{4\alpha_i\alpha_j}, \quad \sum_i \alpha_i = 2\alpha_0. \quad (87)$$

While the global behavior of correlators of vertex operators is affected by the background charge, their local properties are completely encoded in the short-distance operator product expansions (OPE)

$$V_{\alpha_1}(z_1)V_{\alpha_2}(z_2) = (z_1 - z_2)^{2\alpha_1\alpha_2}V_{\alpha_1+\alpha_2}(z_2) + \dots, \quad (88)$$

where the dots stand for subleading terms.

Finally, let us mention that in CFT literature it is customary to label holomorphic charges and weights by two numbers r, s according to

$$\begin{aligned} \alpha_{r,s} &= \frac{1}{2}(1-r)\alpha_+ + \frac{1}{2}(1-s)\alpha_-, \\ h_{r,s} &= \alpha_{r,s}(\alpha_{r,s} - 2\alpha_0) = \frac{1}{4} \left[\left(r\frac{\sqrt{\kappa}}{2} - s\frac{2}{\sqrt{\kappa}} \right)^2 - \left(\frac{\sqrt{\kappa}}{2} - \frac{2}{\sqrt{\kappa}} \right)^2 \right] \\ &= \frac{(r\kappa - 4s)^2 - (\kappa - 4)^2}{16\kappa}. \end{aligned} \quad (89)$$

We stress that we use it as a shorthand notation and do not impose any restrictions on r or s . The holomorphic primary field of weight $h_{r,s}$ is denoted by $\psi_{r,s}(z)$. In the notation (84), this is the field $V_{\alpha_{r,s}}(z)$. The corresponding spinless bulk operator $V^{(\alpha_{r,s})}(z, \bar{z})$ will be denoted as $\psi_{r,s}(z, \bar{z})$.

8.3 Coulomb gas CFT in the upper half plane

We now consider modifications to the Coulomb gas description that result when the boson lives in a bounded region. Due to conformal invariance we may choose the simplest possible case: the upper half plane \mathbb{H} , and most formulas will be written for this case. For basics on boundary CFT see Refs. [19, 63, 64].

First we note that since the boson field φ is defined by the orientation of the loops, it is a pseudoscalar, meaning that it changes sign under parity transformation, or reflection in a boundary ($z \rightarrow \bar{z}$ for the upper half plane). This implies that we must impose the Dirichlet boundary condition

$$\partial_l \varphi|_{\partial D} = 0, \quad (90)$$

where the derivative is taken along the boundary (for \mathbb{H} the boundary is the real axis $z = \bar{z}$). Each boundary is then a level line of φ , in correspondence with lattice loops.

The Dirichlet boundary condition glues together the holomorphic and antiholomorphic sectors of the theory in a way that is easiest to describe in terms of the image charges, see, for example, Chapter 11 in Ref. [19]. The dependence of correlators of primary fields on the antiholomorphic coordinates \bar{z}_i in the upper half plane can be regarded as the dependence on holomorphic coordinates z_i^* in the lower half plane, after the parity transformation is performed. In our case the parity transformation for the chiral boson is simply

$$\bar{\phi}(\bar{z}) \rightarrow -\phi(z^*),$$

which gives the following prescription for bulk vertex operators in the upper half plane:

$$\begin{aligned} V_{e,0}(z, \bar{z}) &= e^{i\sqrt{2}e\varphi(z, \bar{z})} = e^{i\sqrt{2}e[\phi(z) + \bar{\phi}(\bar{z})]} \rightarrow e^{i\sqrt{2}e\phi(z)} e^{-i\sqrt{2}e\phi(z^*)}, \\ V_{0,m}(z, \bar{z}) &= e^{-\sqrt{2}m\tilde{\varphi}(z, \bar{z})} = e^{i\sqrt{2}m[\phi(z) - \bar{\phi}(\bar{z})]} \rightarrow e^{i\sqrt{2}m\phi(z)} e^{i\sqrt{2}m\phi(z^*)}, \\ V_{e,m}(z, \bar{z}) &\rightarrow e^{i\sqrt{2}(m+e)\phi(z)} e^{i\sqrt{2}(m-e)\phi(z^*)}, \\ V_{\alpha, \bar{\alpha}}(z, \bar{z}) &= e^{i\sqrt{2}\alpha\phi(z)} e^{i\sqrt{2}\bar{\alpha}\bar{\phi}(\bar{z})} \rightarrow e^{i\sqrt{2}\alpha\phi(z)} e^{-i\sqrt{2}\bar{\alpha}\phi(z^*)}. \end{aligned} \quad (91)$$

The right hand sides of these equations should be viewed as products of two holomorphic operators.

This situation can be summarized by saying that under reflection the electric charges change sign, while the magnetic ones do not. This implies, in particular, that on the boundary (the real axis) only magnetic operators survive, electric ones being rendered trivial by the Dirichlet boundary condition. Indeed, as z and z^* both approach a point x on the real axis, the bulk operator $V_{e,m}(z, \bar{z})$ (with any electric charge e) reduces to

$$V^{(2m)}(x) = e^{i2\sqrt{2}m\phi(x)}. \quad (92)$$

Such boundary operator is characterized only by one weight which is the same as the holomorphic weight $h(0, 2m)$ of a bulk operator. This situation can also be described by saying that the fusion on the boundary of a holomorphic operator with its image produces a magnetic boundary operator.

8.4 Creation of critical curves

As we have seen, in a microscopic description a critical curve starting at a boundary is created by a change in boundary conditions. In the effective language of CFT such change is implemented by insertion of a certain operator at a point on the boundary.

Microscopic definition of height function H implies that if we have n critical curve with the same orientation that start on a boundary at some point, the boundary values of the field φ on the two sides of the point should differ by $\pm n\pi\mathcal{R}$. The curves should be oriented in the same way to prevent them from reconnecting with each other. For a system on the UHP, n such curves starting at the origin are then created by the following boundary condition:

$$\varphi(x) = \begin{cases} n\pi\mathcal{R}, & x \leq 0, \\ 0, & x > 0. \end{cases} \quad (93)$$

The operator creating such a jump in the value of φ at $x = 0$ is a certain magnetic boundary operator. To find out what it is, we first consider magnetic operators in the bulk.

Note that the insertion of a magnetic operator in the bulk creates a vortex in the field φ . Indeed, the bulk OPE (88) gives

$$\begin{aligned} V_{e,0}(z, \bar{z})V_{0,m}(z', \bar{z}') &= \left(\frac{z - z'}{\bar{z} - \bar{z}'}\right)^{2em} V_{e+m}(z')\bar{V}_{e-m}(\bar{z}') + \dots \\ &= e^{4iem \arg(z-z')} V_{e+m}(z')\bar{V}_{e-m}(\bar{z}') + \dots \end{aligned}$$

This means that when z goes around z' , the field φ changes by $4\sqrt{2}\pi m$, and hence, a discontinuity line with this jump arises, see Fig. 13. If this vortex corresponds to a star of n critical curves joined at the point z' , the change in φ should be equal to $n\pi\mathcal{R}$, and then the discontinuity is not physical due to the compactification of φ . This gives the magnetic charge of the bulk curve creating operator:

$$m = \frac{\sqrt{2}}{8}n\mathcal{R} = \frac{n}{2\sqrt{\kappa}} = -\frac{n}{4}\alpha_-, \quad (94)$$

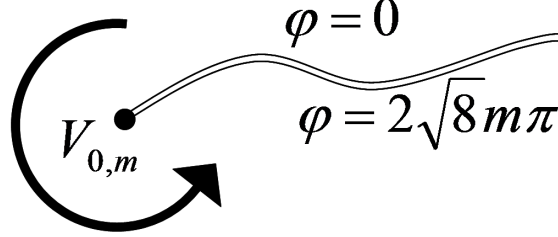


Figure 13: A bulk magnetic operator $V_{0,m}$ creates a vortex configuration of the field φ . The field changes by $2\sqrt{8}\pi m$ when going around $V_{0,m}$.

where we used the value (75) of the compactification radius and the definition (77) of α_- . In order to be spinless (otherwise the operator would transform under rotations, giving non-trivial dependence on the winding number of curves), the bulk curve creating operator should also have electric charge α_0 .

We have, therefore, found the holomorphic charge of the bulk curve creation operator to be

$$\alpha = \alpha_0 - \frac{n}{4}\alpha_- = \alpha_{0,n/2}$$

in the notation of Eq. (89). The operator itself is then $\psi_{0,n/2}(z, \bar{z})$, and its holomorphic weight is

$$h_{0,n/2} = \frac{4n^2 - (\kappa - 4)^2}{16\kappa}.$$

In particular, a single critical curve going through a point z is created by the operator $\psi_{0,1}(z, \bar{z})$ with the holomorphic weight $h_{0,1} = (8 - \kappa)/16$. Notice that this weight is related to the fractal dimension of the critical curve by $d_f = 2 - 2h_{0,1}$, see Ref. [65] for details.

Now we go back to the boundary. According to Eq. (91), as z approaches a point x on the real axis, the bulk operator $V_{e,m}(z, \bar{z})$ (with any electric charge e) reduces to $e^{i2\sqrt{2}m\phi(x)}$. In this process the two sides of the discontinuity line become parts of the real axis separated by x (see Fig. 14). Thus, when we go from one side of x to the other along a semicircle, the field changes by the same amount as in making a full circle around a bulk magnetic operator. Then to create the boundary condition (93), and, correspondingly, n critical curves starting at the origin, we need to insert there the magnetic operator

$$V^{(m)}(x) = e^{i\sqrt{2}m\phi(x)},$$

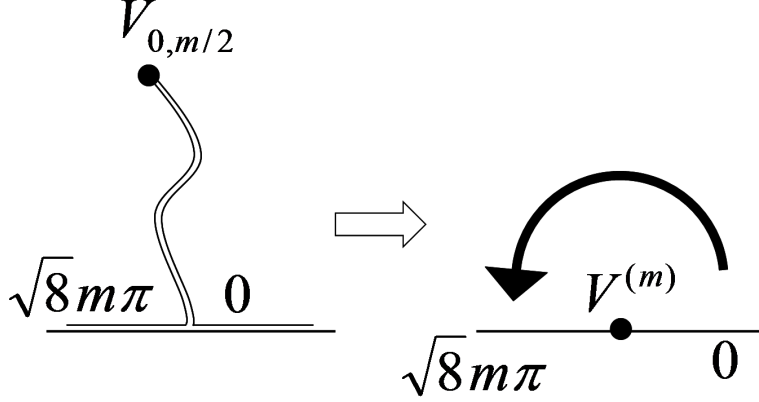


Figure 14: A boundary magnetic operator is obtained as the boundary limit of the bulk magnetic operator $V_{0,m/2}$.

with the magnetic charge determined by the condition $\sqrt{8\pi}m = n\pi\mathcal{R}$, which gives

$$m = \frac{1}{\sqrt{8}}n\mathcal{R} = \frac{n}{\sqrt{\kappa}} = -\frac{n}{2}\alpha_-. \quad (95)$$

In the notation of Eq. (89) this is $\alpha_{1,n+1}$, so the boundary curve creating operator is $\psi_{1,n+1}(x)$ with dimension

$$h_{1,n+1} = \frac{2n^2 + n(4 - \kappa)}{2\kappa}.$$

In particular, a single curve is created by the insertion of $\psi_{1,2}(x)$ with the dimension

$$h_{1,2} = \frac{6 - \kappa}{2\kappa}, \quad (96)$$

which appeared before in the discussion of restriction property of SLE, see Eq. (54).

9 Harmonic measure of critical curves

Harmonic measure is a useful quantity describing geometry of complicated plane domains [66, 67]. In the following sections I define it and the related spectrum of multifractal exponents, and then show how to compute these exponents for harmonic measure on critical curves using CFT.

9.1 Definitions of harmonic measure

Let D be a domain (an open connected subset of the complex plane), ∂D its boundary, and $z \in D$.

Harmonic measure in D from z , denoted as $\omega_D(z, \Gamma)$ where $\Gamma \in \partial D$, is a probability measure on ∂D , which can be defined as the probability that the standard two-dimensional Brownian motion B_t that starts at z hits ∂D in a given portion $\Gamma \subset \partial D$ of the boundary:

$$\omega_D(z, \Gamma) = \mathbf{P}^z[B_{\tau_D} \in \Gamma].$$

Here τ_D is the escape time from D , that is, the first time when the Brownian motion B_t hits the boundary ∂D .

Harmonic measure $\omega_D(z, \Gamma)$ can also be characterized as the unique harmonic function (solution of the Laplace's equation) $u(z)$ in D with the Dirichlet boundary conditions

$$u(\zeta) = 1, \quad \zeta \in \Gamma, \quad u(\zeta) = 0, \quad \zeta \notin \Gamma.$$

Here we will only be interested in harmonic measure from infinity of the domain D exterior to a closed curve γ . In this case we will denote it simply by $\omega(\Gamma)$. Harmonic measure $\omega(\Gamma)$ has an electrostatic interpretation. Imagine that D is a charged metallic cluster with the total charge one. The charge is concentrated on the boundary ∂D . Then $\omega(\Gamma)$ is the charge located on the portion Γ of ∂D .

Harmonic measure is conformally-invariant: if $f : D \rightarrow D'$ is a conformal map that is continuous and one-to-one on $D \cup \partial D$, then

$$\omega_D(z, \Gamma) = \omega_{D'}(f(z), f(\Gamma)).$$

9.2 Moments of harmonic measure and multifractal spectrum

Consider a closed curve γ . One can cover the curve γ with discs $B(z_i, r)$ of radius r centered at some points $z_i \in \gamma$ (z_i form a discrete subset of γ). Let

$$p(z_i, r) = \omega(\gamma \cap B(z_i, r))$$

be the harmonic measure (from infinity) of the portion of the curve covered by the disc $B(z_i, r)$. Then we consider the moments

$$M_h = \sum_{i=1}^N p(z_i, r)^h, \tag{97}$$

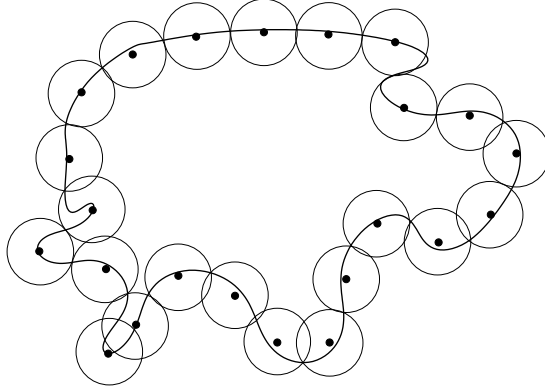


Figure 15: A curve covered by discs.

where h is a real power, and N is the number of discs needed to cover γ . As the radius r gets smaller and the number of discs N gets larger, these moments scale as

$$M_h \sim \left(\frac{r}{L}\right)^{\tau(h)}, \quad \frac{r}{L} \rightarrow 0. \quad (98)$$

The size L (diameter) of the curve is used to make the right hand side of this equation dimensionless.

The function $\tau(h)$ is called the **multifractal spectrum** of the curve γ . This function encodes a lot of information of the curve γ . It also has some simple properties. First of all, since all $0 < p(z_i, r) \leq 1$, the moments M_h are well defined for any real h , and the function $\tau(h)$ is non-decreasing: $\tau(h) \leq \tau(h')$ for any $h < h'$. Secondly, if $h = 1$, the sum in (97) is equal to the total charge of the cluster, and therefore does not scale with r , producing the normalization condition

$$\tau(1) = 0.$$

Third, if we set $h = 0$, M_0 is simply the number N of discs of radius r necessary to cover the curve γ , so that by definition the fractal (Hausdorff) dimension of γ is

$$d_f = -\tau(0).$$

If the curve γ were smooth, we would have a simple relation $\tau(h) = h - 1$. For a fractal curve one defines the anomalous exponents $\delta(h)$ by

$$\tau(h) = h - 1 + \delta(h).$$

Also, the generalized multifractal dimensions of a fractal curve γ are defined as $D(h) = \tau(h)/(h - 1)$ (so that $D(0) = d_f$). A non-trivial theorem due to N. Makarov [68, 69] states that

$$D(1) = \tau'(1) = 1.$$

If the curve γ is a member of an ensemble of curves generated in some random way, the moments M_h become random variables, and we can study their distribution functions. If the distribution functions are narrow, then the mean moments $\overline{M_h}$, where the overline denotes the ensemble averaging, characterize them well. This is usually the case for $|h|$ that is not too large. In this case the mean and the typical moments scale in the same way, which is a statement about self-averaging of the moments. This is what we assume here.

In this situation it is also natural to assume some sort of ergodicity, meaning that the summation over the points z_i in Eq. (97) for a typical curve is equivalent to the ensemble average. Hence we can write

$$M_h = N \overline{p(z_0, r)^h} \sim \left(\frac{r}{L}\right)^{\tau(0)} \overline{p(z_0, r)^h},$$

where now the harmonic measure $p(z_0, r)$ is evaluated at any point $z_0 \in \gamma$. We define the local multifractal exponent $\tilde{\tau}(h)$ at a point z_0 by

$$\overline{p(z_0, r)^h} \sim \left(\frac{r}{L}\right)^{\tilde{\tau}(h)}. \quad (99)$$

Similar to $\tau(h)$, for a smooth curve we have $\tilde{\tau}(h) = h$, so in general we define the local anomalous exponents $\Delta_{\text{bulk}}^{(2)}(h)$ by

$$\tilde{\tau}(h) = h + \Delta_{\text{bulk}}^{(2)}(h).$$

The reason for the superscript (2) and the subscript “bulk” will become clear in the next subsection.

It is obvious from the definitions that $\tilde{\tau}(0) = \Delta_{\text{bulk}}^{(2)}(0) = 0$, and we deduce simple ergodicity relations

$$\begin{aligned} \tilde{\tau}(h) &= \tau(h) - \tau(0), & \tau(h) &= \tilde{\tau}(h) - \tilde{\tau}(1), \\ \Delta_{\text{bulk}}^{(2)}(h) &= \delta(h) - \delta(0), & \delta(h) &= \Delta_{\text{bulk}}^{(2)}(h) - \Delta_{\text{bulk}}^{(2)}(1), \\ d_f &= 1 + \Delta_{\text{bulk}}^{(2)}(1). \end{aligned} \quad (100)$$

9.3 Critical curves and uniformizing maps

So far we have considered arbitrary closed curves. An example of such a curve is the exterior perimeter γ of a critical cluster. One can imagine that the cluster is made of a conducting material and carries the total unit electric charge. The harmonic measure of any part of γ is then equal to the electric charge of this part. Since exterior perimeters are always dilute curves in the sense of Section 8.1 (see also discussion of duality around Eq. (19)), in the remaining part of this paper we will always assume $\kappa \leq 4$.

The critical clusters and their boundaries appear as members of statistical ensembles, which is the situation suitable for local multifractal analysis of the previous section. We then will pick a point of interest z_0 on the curve γ and consider a disc of a small radius $r \ll L$ centered at z_0 . It surrounds a small part of γ , and we will study the mean moments of the harmonic measure $p(z_0, r)$ and their scaling as in Eq. (99).

There are a few generalizations of the simple closed critical curve considered above. First of all, the curve γ need not be closed or stay away from system boundaries. If γ touches a boundary, we can supplement it with the image $\bar{\gamma}$ (reflected in the boundary) and take the union $\gamma \cup \bar{\gamma}$ to be the charged conducting object. The electrostatic definition of $p(z_0, r)$ can be naturally extended to the cases when z_0 is the endpoint of n critical curves on the boundary or in the bulk. If n is even, the latter case can be also seen as $n/2$ critical curves passing through z_0 . In particular, $n = 2$ corresponds to the situation of a single curve in the bulk, considered above.

When z_0 is the endpoint of n critical curves on the boundary or the bulk we define the corresponding scaling exponents similar to Eq. (99):

$$\overline{p(z_0, r)^h} \sim r^{h+\Delta^{(n)}(h)}, \quad \overline{p(z_0, r)^h} \sim r^{h+\Delta_{\text{bulk}}^{(n)}(h)}. \quad (101)$$

In the case of a single curve we will drop the superscript, so, for example, $\Delta(h) \equiv \Delta^{(1)}(h)$ is the same exponent as obtained in Eq. (71).

These exponents were first obtained by means of quantum gravity in [2, 3]. For a critical system with parameter κ the results read

$$\Delta(h) = \frac{\kappa - 4 + \sqrt{(\kappa - 4)^2 + 16\kappa h}}{2\kappa} = \frac{\sqrt{1 - c + 24h} - \sqrt{1 - c}}{\sqrt{25 - c} - \sqrt{1 - c}}, \quad (102)$$

$$\Delta^{(n)}(h) = n\Delta(h), \quad (103)$$

$$\Delta_{\text{bulk}}^{(n)}(h) = -\frac{h}{2} + \left(\frac{1}{16} + \frac{n-1}{4\kappa}\right)(\kappa - 4 + \sqrt{(\kappa - 4)^2 + 16\kappa h}). \quad (104)$$

Remarkably, $\Delta(h)$ is the gravitationally dressed dimension h , as given by the KPZ formula of 2D quantum gravity [4, 70]. Starting in the next section,

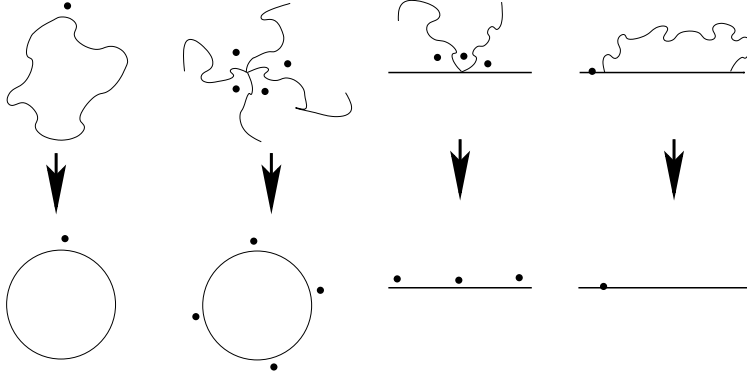


Figure 16: The uniformizing conformal maps for various cases considered. The dots denote that points where the electric field is measured.

we will show how to obtain these exponents in the framework of Coulomb gas CFT, where they are also written in a more transparent way.

The basic property that allows to calculate the multifractal exponents using CFT is the conformal invariance of the harmonic measure. Let us consider a conformal map $w(z)$ of the exterior of γ to a standard domain. Usually we will choose the upper half plane but sometimes the exterior of a unit circle is more convenient. We normalize the map so that the point of interest z_0 is mapped onto itself, choose it to be the origin $z_0 = 0$ and demand that at infinity $w(z) = z + o(z)$. Examples of $w(z)$ for several cases are shown in Fig. 16.

The scaling of $w(z)$ near the origin is directly related to that of the harmonic measure. Indeed, since $p(0, r)$ is the charge inside the disc of radius r , by Gauss theorem it is equal to the flux of the electric field through the boundary of this disc. This, in turn, should scale as the circumference of this disc times a typical absolute value of the electric field at the distance r from the origin, i.e. $|w'(r)|$. This leads to scaling relation

$$p(0, r) \sim r|w'(r)|,$$

which allows to rewrite the definitions (101) as

$$\overline{|w'(r)|^h} \sim r^{\Delta^{(n)}(h)}, \quad \overline{|w'(r)|^h} \sim r_{\text{bulk}}^{\Delta_{\text{bulk}}^{(n)}(h)}. \quad (105)$$

The relation of the scaling of the harmonic measure and the derivative of a uniformizing map allows for further generalizations. Namely, we can

measure the electric field in more than one point. Close to the origin n curves divide the plain into n sectors in the bulk and $n + 1$ on the boundary. Then we can study objects like

$$\frac{\overline{|w'(z_1)|^{h_1} \dots |w'(z_{n+1})|^{h_{n+1}}}}{\overline{|w'(z_1)|^{h_1} \dots |w'(z_n)|^{h_n}}} \quad \begin{array}{l} \text{(boundary),} \\ \text{(bulk),} \end{array} \quad (106)$$

where no two z_i 's lie in the same sector. The case when the electric field is not measured in some sectors is done by setting $h_i = 0$ in them. We will see how to express these quantities as CFT correlation functions. In the case when z_i are all at the distance r from the origin ($z_i = r e^{i\theta_i}$, $\theta_i = \text{const}$), these averages scale as $r^{\Delta^{(n)}(h_1, \dots, h_{n+1})}$ and $r^{\Delta_{\text{bulk}}^{(n)}(h_1, \dots, h_n)}$ with the *higher multifractal exponents* [3]

$$\Delta^{(n)}(h_1, \dots, h_{n+1}) = \sum_{i=1}^{n+1} \Delta^{(n)}(h_i) + \frac{\kappa}{2} \sum_{i < j}^{n+1} \Delta(h_i) \Delta(h_j), \quad (107)$$

$$\Delta_{\text{bulk}}^{(n)}(h_1, \dots, h_n) = \sum_{i=1}^n \Delta_{\text{bulk}}^{(n)}(h_i) + \frac{\kappa}{4} \sum_{i < j}^n \Delta(h_i) \Delta(h_j). \quad (108)$$

9.4 Derivative expectations and CFT in fluctuating geometry

Here we begin the Coulomb gas derivation of results (102 – 104, 107, 108). It is easiest to start with a point where a single curve γ connects with the system boundary. We assume that the critical system occupies the upper half plane, so that the real axis is the boundary.

The partition function $Z(0, L)$, restricted to configurations that contain a curve γ connecting the points 0 and L , is given by the correlator of two boundary curve creating operators, in this case $\psi_{1,2}$ (see section (8.4)):

$$\frac{Z(0, L)}{Z} = \langle \psi_{1,2}(0) \psi_{1,2}(L) \rangle_{\mathbb{H}},$$

where Z is the unrestricted partition function. This correlation function can be computed in two steps. In the first step we pick a particular realization of the curve γ . Within each realization, it is the boundary separating two independent systems—the interior and the exterior of γ . In both these systems we can sum over microscopic degrees of freedom to obtain the partition functions Z_{γ}^{int} and Z_{γ}^{ext} , respectively. These are stochastic objects that depend on the fluctuating geometry of γ . In the second step we average over

the ensemble of curves of γ . We thus obtain

$$Z(0, L) = \overline{Z_\gamma^{\text{int}} Z_\gamma^{\text{ext}}}.$$

Next, we insert an additional boundary primary operator $O_h(r)$ of dimension h close to 0, and another one $O_h(\infty)$ at infinity. The first one serves as a “probe” of harmonic measure, and the second is necessary to ensure the charge neutrality. We thus consider the correlation function

$$\langle \psi_{1,2}(0) O_h(r) \psi_{1,2}(L) O_h(\infty) \rangle_{\mathbb{H}}. \quad (109)$$

Since we are only interested in the r -dependence of the correlation function, we can fuse together the distant primary fields: $\psi_{1,2}(L) O_h(\infty) \rightarrow \Psi(\infty)$. We therefore consider the r -dependence of a 3-point function

$$\langle \psi_{1,2}(0) O_h(r) \Psi(\infty) \rangle_{\mathbb{H}}, \quad (110)$$

and show that it yields the statistics of the harmonic measure.

Decomposing the upper half plane into the exterior and the interior of γ as before, we can rewrite (109) as the average over the fluctuating geometry of γ :

$$\overline{\langle O_h(r) O_h(\infty) \rangle_{\gamma^{\text{ext}}} Z_\gamma^{\text{int}} Z_\gamma^{\text{ext}}}. \quad (111)$$

Here the domain of the definition of the correlation function of primary fields is the exterior of γ . This correlation function is statistically independent from the other two factors in the numerator of (111) in the limit $r \ll |L|$, and we are left with the correlation function $\langle O_h(r) O_h(\infty) \rangle_{\gamma^{\text{ext}}}$ of two primary fields of boundary CFT, further averaged over all configurations of the boundary γ . This average is proportional to the 3-point correlation function (110).

Now we apply the conformal transformation $w(z)$ which maps the exterior of γ onto the upper half plane. Being a primary operator of weight h , $O_h(r)$ transforms as $O_h \rightarrow |w'(r)|^h O_h(w(r))$, while $O_h(\infty)$ does not change because of the normalization of $w(z)$ at infinity. The transformation relates the correlation function in the exterior of γ to a correlation function in the upper half plane:

$$\langle O_h(r) O_h(\infty) \rangle_{\gamma^{\text{ext}}} = |w'(r)|^h \langle O_h(w(r)) O_h(\infty) \rangle_{\mathbb{H}}. \quad (112)$$

The latter does not depend on r and can be neglected.

Summing up, we obtain a scaling relation between the moments of the harmonic measure near the boundary and correlation functions of primary boundary fields [33]:

$$|\overline{w'(r)}|^h \propto \langle O_h(r)\psi_{1,2}(0)\Psi(\infty)\rangle_{\mathbb{H}}, \quad r \ll |L|. \quad (113)$$

The primary field $\Psi(\infty)$ should be chosen in such a way as to render the correlation function non-zero. The choice is made unique by picking the conformal block which satisfies simple physical condition $\Delta(0) = 0$. The r -dependence of the correlation function (113) is found from the OPE of the fields $O_h(r)$ and $\psi_{1,2}(0)$:

$$O_h(r)\psi_{1,2}(0) = \sum_{k=1}^{\infty} r^{\Delta_k} \Phi^{(k)}(0). \quad (114)$$

The exponent $\Delta(h)$ is then identified as the lowest power Δ_k such that $\langle \Phi^{(k)}(0)\Psi(\infty)\rangle \neq 0$.

Several remarks are in order. As presented, this argument produces the scaling exponent $\Delta(h)$ for a single curve on the boundary. But it can be easily modified for studying the scaling behavior in all other cases. The case of n curves starting from a point on the boundary is obtained by simple replacement of the curve creating operators: $\psi_{1,2} \rightarrow \psi_{1,n+1}$ (see Section (8.4)).

Also, the argument can be repeated for the case of γ connected to the real axis only at one point (as in SLE). In this case no separation in two systems is necessary. Finally, nothing compels us measure the electric field on the real axis. We could take instead a bulk primary field $O_{h',h'}(z, \bar{z})$, where $|z| = r$. The weight h' should be chosen such that when the holomorphic part $O_{h'}(z)$ is fused with its image $O_{h'}(z^*)$, the boundary field $O_h(\frac{z+z^*}{2})$ with dimension h is obtained, similar to Eq. (92). This fusion will be used below.

9.5 Calculation of boundary multifractal exponents

In practice we view both O_h and $\psi_{1,2}$ in Eq. (114) as boundary vertex operators $V^{(\alpha_h)}$ and $V^{(\alpha_{1,2})}$, see Eq. (92), with charges

$$\alpha_h = \alpha_0 - \sqrt{\alpha_0^2 + h}, \quad \alpha_{1,2} = -\frac{\alpha_-}{2} = \frac{1}{\sqrt{\kappa}}.$$

The leading term in the OPE of these two operators corresponds to simple addition of charges, see Eq. (88). Hence, the scaling relation (113) immediately gives the result (102) written in a compact and suggestive form:

$$\Delta(h) = 2\alpha_{1,2}\alpha_h. \quad (115)$$

It is interesting that written in this form, the KPZ formula for gravitationally dressed dimensions amounts to OPE of vertex operators in a simple Coulomb gas CFT, without any quantum gravity.

An immediate generalization to the statistics of harmonic measure of n curves reaching the system boundary at the same point is obtained by replacing $\psi_{1,2} \rightarrow \psi_{1,n+1}$. Since $\alpha_{1,n+1} = -n\alpha_-/2 = n\alpha_{1,2}$, this immediately leads to

$$\Delta^{(n)}(h) = 2\alpha_{1,n+1}\alpha_h = n\Delta(h),$$

which is the same as Eq. (103).

To calculate the higher boundary multifractal exponents, we consider n non-intersecting critical curves growing from the origin on the boundary (the real axis). It will be convenient to assume that the curves end somewhere in the bulk thus forming a boundary star (e.g. the third picture in Fig. 16). Let $w(z)$ be the conformal map of the exterior of the star to the upper half plane with the usual normalization $w(z) = z + o(z)$ at $z \rightarrow \infty$.

We want to find the scaling of the average

$$\overline{|w'(z_1)|^{h_1} \dots |w'(z_{n+1})|^{h_{n+1}}},$$

where z_i are all close to the origin, no two of them lying in the same sector. The latter condition will be automatically satisfied in the subsequent calculation due to the following: if in a particular realization two points z_i and z_j happen to be in the same sector, then $w(z_i) - w(z_j) \rightarrow 0$ as $z_i - z_j \rightarrow 0$, but if they lie in different sectors, $w(z_i) - w(z_j)$ remains large in the same limit.

Since n curves starting from the origin on the boundary are produced by the operator $\psi_{1,n+1}(0)$, we now consider a boundary CFT correlation function with several ‘‘probes’’ of the harmonic measure:

$$C = \left\langle \prod_{i=1}^{n+1} O_{h'_i, h'_i}(z_i, \bar{z}_i) \psi_{1,n+1}(0) \Psi(\infty) \right\rangle_{\mathbb{H}}. \quad (116)$$

The primary field at infinity represents the fusion of all fields far from the origin and should be chosen by the charge neutrality condition. As before,

this correlation function is equal to the statistical average of a certain correlator in the fluctuating domain, and we further apply the uniformizing map $w(z)$ to transform this domain into the UHP:

$$C = \overline{\prod_i |w'(z_i)|^{2h'_i} \langle \prod_i O_{h'_i, h'_i}(w(z_i), \bar{w}(\bar{z}_i)) \Psi(\infty) \rangle_{\mathbb{H}}}. \quad (117)$$

Unlike Eq. (112), the correlator under the average cannot be neglected since it does depend on the short scale r , as we shall see soon.

The correlator C can now be evaluated in two ways. As before, we view the primaries $O_{h'_i, h'_i}(z_i, \bar{z}_i)$ as vertex operators with charges

$$\alpha'_i = \alpha_0 - \sqrt{\alpha_0^2 + h'_i}. \quad (118)$$

Then, using the prescription (91), we can rewrite C in Eq. (116) as a full plane chiral correlator, which then is evaluated using Eq. (86):

$$\begin{aligned} C &= \langle \prod_i O_{h'_i}(z_i) O_{h'_i}(z_i^*) \psi_{1, n+1}(0) \Psi(\infty) \rangle \\ &\propto \prod_i |z_i|^{2\alpha_{1, n+1} \alpha'_i} \prod_{i < j} |z_i - z_j|^{4\alpha'_i \alpha'_j} \prod_{i, j} (z_i - z_j^*)^{2\alpha'_i \alpha'_j}. \end{aligned}$$

When all z_i are at the same distance r from the origin, the last expression scales as

$$C \propto r^{4\alpha_{1, n+1} \sum_i \alpha'_i + 8 \sum_{i < j} \alpha'_i \alpha'_j + 2 \sum_i \alpha_i'^2}. \quad (119)$$

On the other hand, we can evaluate the correlator that appears inside the average in Eq. (117) in the same way:

$$\begin{aligned} \langle \prod_i O_{h'_i, h'_i}(w(z_i), \bar{w}(\bar{z}_i)) \Psi(\infty) \rangle_{\mathbb{H}} &= \langle \prod_i O_{h'_i}(w(z_i)) O_{h'_i}(w^*(z_i)) \Psi(\infty) \rangle \\ &\propto \prod_i (w(z_i) - w^*(z_i))^{2\alpha_i'^2} \prod_{i < j} |w(z_i) - w(z_j)|^{4\alpha'_i \alpha'_j} \prod_{i \neq j} (w(z_i) - w(z_j^*))^{2\alpha'_i \alpha'_j}. \end{aligned}$$

We specifically separated the diagonal ($i = j$) terms, since only they contribute to the necessary short-distance behavior. All the other terms insure that the realizations of the curves in which any two points z_i end up in the same sector are suppressed (since the distances $w(z_i) - w(z_j)$ are then small), and we can consider only the case when all $w(z_i)$ are far apart. Then the relevant short-distance dependence of Eq. (117) is

$$C \propto \overline{\prod_i |w'(z_i)|^{2h'_i} (w(z_i) - w^*(z_i))^{2\alpha_i'^2}}.$$

Insofar as the scaling with r is concerned, we further approximate $w(z_i) - w^*(z_i) \sim |z_i| |w'(z_i)| \sim r |w'(z_i)|$. This gives

$$C \propto r^{2 \sum_i \alpha_i'^2} \prod_i \overline{|w'(z_i)|^{2h_i' + 2\alpha_i'^2}}. \quad (120)$$

The exponents in the last factor

$$2h_i' + 2\alpha_i'^2 = 2\alpha_i'(\alpha_i' - 2\alpha_0) + 2\alpha_i'^2 = 2\alpha_i'(2\alpha_i' - 2\alpha_0) = h_{\alpha_i} = h_i$$

are the dimensions of the boundary operators with charges

$$\alpha_i = 2\alpha_i' = \alpha_0 - \sqrt{\alpha_0^2 + h_i},$$

appearing in the OPE of two chiral operators with charges α_i' .

Finally, comparing Eqs. (119) and (120), we get the result

$$\overline{|w'(z_1)|^{h_1} \dots |w'(z_{n+1})|^{h_{n+1}}} \propto r^{\Delta^{(n)}(h_1, \dots, h_{n+1})},$$

with the higher multifractal exponent

$$\Delta^{(n)}(h_1, \dots, h_{n+1}) = 2\alpha_{1, n+1} \sum_{i=1}^{n+1} \alpha_i + 2 \sum_{i < j}^{n+1} \alpha_i \alpha_j,$$

which is the formula (107).

9.6 Calculation of bulk multifractal exponents

Calculation of bulk multifractal behavior is done in much the same way as on the boundary, so we go straight to the general case of higher bulk exponents.

Let the critical system, occupying the whole complex plane, be restricted to having n critical curves growing from a single point, in which we place the origin $z = 0$. We will assume that $z = 0$ is the only common point of these curves, since the local results around this points are unaffected by the curves' behavior at large distances. We define the conformal map $w(z)$ of the exterior of the “star” to the exterior of a unit circle with the the normalization $w(z) = z + o(z)$ at $z \rightarrow \infty$.

Close to the origin the curves divide the plane into n sectors. We consider a quantity

$$\overline{|w'(z_1)|^{h_1} \dots |w'(z_n)|^{h_n}},$$

where z_i are points close to the origin, no two of them lying in one sector. As before, if two points z_i and z_j happen to be in the same sector, $w(z_i) - w(z_j) \rightarrow 0$ when $z_i - z_j \rightarrow 0$, but if they lie in different sectors, $w(z_i) - w(z_j)$ remains large.

Since n curves starting from the origin in the bulk are produced by the operator $\psi_{0,n/2}(0)$, we introduce a CFT correlation function

$$C_{\text{bulk}} = \left\langle \prod_{i=1}^n O_{h'_i, h'_i}(z_i, \bar{z}_i) \psi_{0,n/2}(0) \Psi(\infty) \right\rangle, \quad (121)$$

where, as before, h'_i is the weight of a primary field such that the result of its fusion with its image has the weight h_i :

$$\alpha_i = 2\alpha'_i.$$

Proceeding exactly as in the boundary case, we first rewrite the correlator C_{bulk} as the ensemble average of another correlator in the exterior of the star of critical curves. Then we map that exterior to the exterior of a unit disk $\mathbb{C} \setminus D$ (see the second picture on Fig. 16):

$$C_{\text{bulk}} = \overline{\prod_i |w'(z_i)|^{2h'_i} \left\langle \prod_i O_{h'_i, h'_i}(w(z_i), \bar{w}(\bar{z}_i)) \Psi(\infty) \right\rangle_{\mathbb{C} \setminus D}}. \quad (122)$$

Next, we evaluate C_{bulk} as defined in Eq. (121), using Eq. (87):

$$C_{\text{bulk}} = \prod_i |z_i|^{4\alpha_{0,n/2}\alpha'_i} \prod_{i<j} |z_i - z_j|^{4\alpha'_i\alpha'_j} \propto r^{4\alpha_{0,n/2} \sum_i \alpha'_i + 4 \sum_{i<j} \alpha'_i\alpha'_j}.$$

Alternative evaluation starting from Eq. (122) gives the same result as Eq. (120). Combining the two results for C_{bulk} , we obtain

$$\overline{|w'(z_1)|^{h_1} \dots |w'(z_n)|^{h_n}} \propto r^{\Delta_{\text{bulk}}^{(n)}(h_1, \dots, h_n)},$$

with the higher bulk exponent

$$\Delta_{\text{bulk}}^{(n)}(h_1, \dots, h_n) = \sum_{i=1}^n \Delta_{\text{bulk}}^{(n)}(h_i) + \sum_{i<j}^n \alpha_{h_i} \alpha_{h_j},$$

where

$$\Delta_{\text{bulk}}^{(n)}(h) = 2\alpha_{0,n/2}\alpha_h - \frac{1}{2}\alpha_h^2 = (2\alpha_{0,n/2} - \alpha_0)\alpha_h - \frac{h}{2}$$

is the scaling exponent of a single $\overline{|w'(z)|^h}$ in the presence of n critical curves in the bulk. These are the results quoted in Eqs. (104, 108).

10 Omitted topics: guide to the literature

The current literature on SLE and related subject is already quite large. In this paper I had to omit many interesting and important topics. In this section I simply list the topics and give appropriate references.

For the overall logic of this paper the biggest omission is the discussion of the relation of SLE and CFT through the identification of CFT correlators and SLE martingales. This identification was established and developed by Bauer and Bernard (see review [5] and references there). We have further developed this correspondence [21], showing that one can recover all familiar objects of the Coulomb gas CFT, such as bosonic field, its current, vertex operators, and the stress-energy tensor, by focusing on SLE martingales. Alternative and independent versions of SLE-CFT correspondence and generalizations were given by Friedrich, Kalkkinen and Kontsevich, see Refs. [51, 52, 71].

Chordal SLE considered in this paper has been generalized in many ways. First of all, one can define SLE in other simply-connected geometries than that of the UHP. The corresponding processes are known as radial SLE [11, 72], whole plane SLE [11], dipolar SLE [65, 73]. All these variants happen to be closely related [74].

Secondly, one can consider SLE in multiply-connected domains including arbitrary Riemann surfaces [51, 52, 75, 76, 77, 78, 79], though there is some amount of arbitrariness involved in the definition, since in this setting the conformal type of the domain changes during the evolution (one moves in the moduli space) [80].

Third, there is a way to modify the dynamics of the growth of a random curve by including certain moving points (“spectators”) on the boundary of the domain, that influence the evolution by supplying a drift term in the (analog of) Loewner equation. This generalization is known as $SLE_{\kappa, \rho}$, where ρ stands for a vector of parameters describing the coupling of the “spectators” [48, 56, 57, 58, 81, 82, 83, 84].

The fourth generalization allows for multiple curves to grow simultaneously. This is called multiple SLE [85, 86, 87, 88, 89, 90].

We can also generalize SLE by dropping the demand that the forcing stochastic function be continuous, but keeping the requirement of stationary and statistically-independent increments. This leads to a much broader class of forcing processes including, in particular, the so called Lévy processes. This generalization might be a useful description of tree-like stochastic growth [34, 91].

Still another generalization is to combine the evolution of conformal

maps with some stochastic process in a Lie algebra or some other algebraic structure. This leads to generalized SLE processes describing CFT with additional symmetries, such as Wess-Zumino models [92, 93].

Recently, a few papers appeared that used SLE as a tool to probe conformal invariance in systems that are not described by traditional statistical mechanics models. A remarkable example is Ref. [94] which numerically demonstrated that zero vorticity lines in highly developed 2D turbulence are SLE_6 with high accuracy. Similar conclusions were presented for domain walls in spin glasses [95] and nodal domains of some chaotic maps [96].

Finally, I would like to mention that there is generalization of Loewner equation that describes evolving 2D domains which may grow with a specified rate at every point on the boundary. These are called Loewner chains (see Refs. [5, 6] for a review of this enormous field in relation to SLE) and can describe various non conformally-invariant growth processes such as Laplacian growth, diffusion-limited aggregation, dielectric breakdown, etc.

Acknowledgements

First I want to thank my collaborators on the projects related to this article: E. Bettelheim, L. Kadanoff, P. Oikonomou, I. Rushkin, and P. Wiegmann.

Other people generously shared their ideas and knowledge of SLE and related things with me, and I thank them all: M. Bauer, M. K. Berkenbusch, D. Bernard, J. Cardy, B. Duplaniter, W. Kager, B. Nienhuis, O. Schramm, and S. Sheffield.

Additional thanks go to the following people who kindly permitted me to use figures from their papers and reviews: M. Bauer, D. Bernard, L. Kadanoff, W. Kager, B. Nienhuis, and W. Werner.

This work was supported by the NSF MRSEC Program under DMR-0213745, the NSF Career award DMR-0448820, the Sloan Research Fellowship from Alfred P. Sloan Foundation, and the Research Innovation Award from Research Corporation.

References

- [1] O. Schramm, Scaling limits of loop-erased random walks and uniform spanning trees, *Israel J. Math.* **118**, 221 (2000); arXiv: math.PR/9904022.
- [2] B. Duplantier, Conformally invariant fractals and potential theory, *Phys. Rev. Lett.* **84**, 1363 (2000).
- [3] B. Duplantier, Conformal fractal geometry and boundary quantum gravity, in *Fractal geometry and applications: a jubilee of Benot Mandelbrot, Part 2*, 365, Proc. Sympos. Pure Math., 72, Part 2, AMS, 2004; arXiv: math-ph/0303034.
- [4] V. G. Knizhnik, A. M. Polyakov and A. B. Zamolodchikov, Fractal structure of 2d-quantum gravity, *Mod. Phys. Lett. A* **3**, 819 (1988).
- [5] M. Bauer and D. Bernard, Loewner chains, in *String theory: from gauge interactions to cosmology*, 41, NATO Sci. Ser. II Math. Phys. Chem., **208**, Springer, Dordrecht, (2006); arXiv: cond-mat/0412372.
- [6] M. Bauer and D. Bernard, 2D growth processes: SLE and Loewner chains, arXiv: math-ph/0602049.
- [7] J. Cardy, Conformal invariance in percolation, self-avoiding walks and related problems, arXiv: cond-mat/0209638.
- [8] J. Cardy, SLE for theoretical physicists, *Ann. Phys.* **318**, 81 (2005); arXiv: cond-mat/0503313.
- [9] I. A. Gruzberg and L. P. Kadanoff, The Loewner equation: maps and shapes, *J. Stat. Phys.* **114**, 1183 (2004); arXiv: cond-mat/0309292.
- [10] W. Kager, B. Nienhuis, A guide to stochastic loewner evolution and its applications, *J. Stat. Phys.* **115**, 1149 (2004); arXiv: math-ph/0312056.
- [11] G. F. Lawler, *Conformally invariant processes in the plane*. Mathematical Surveys and Monographs, 114. American Mathematical Society, Providence, RI, 2005.
- [12] G. F. Lawler, Conformally invariant processes in the plane, available online at URL <http://www.math.cornell.edu/~lawler/papers.html>

- [13] G. F. Lawler, An introduction to the stochastic Loewner evolution, in *Random walks and geometry*, 261, Walter de Gruyter GmbH & Co. KG, Berlin 2004; available online at URL <http://www.math.cornell.edu/~lawler/papers.html>
- [14] O. Schramm, Scaling limits of random processes and the outer boundary of planar Brownian motion, *Current developments in mathematics*, 2000, 233, Int. Press, Somerville, MA, 2001.
- [15] O. Schramm, Conformally invariant scaling limits (an overview and a collection of problems), to appear in the ICM 2006 Madrid Proceedings, arXiv: math.PR/0602151.
- [16] S. Sheffield, Gaussian free fields for mathematicians, arXiv: math.PR/0312099.
- [17] W. Werner, Random planar curves and Schramm-Loewner evolutions, in *Lectures on probability theory and statistics*. Lecture Notes in Mathematics, **1840**. Springer-Verlag, Berlin, 2004; arXiv: math.PR/0303354.
- [18] W. Werner, Conformal restriction and related questions, arXiv: math.PR/0307353.
- [19] P. Di Francesco, P. Mathieu, D. Senechal, *Conformal field theory*, Springer, 1999.
- [20] E. Bettelheim, I. Rushkin, I. A. Gruzberg, and P. Wiegmann, On harmonic measure of critical curves, *Phys. Rev. Lett.* **95**, 170602 (2005); arXiv: hep-th/0507115.
- [21] I. Rushkin, E. Bettelheim, I. A. Gruzberg, and P. Wiegmann, Critical curves in conformally invariant statistical systems, in preparation.
- [22] B. Nienhuis, Coulomb gas formulation of 2D phase transitions, in *Phase Transitions and Critical Phenomena*, vol. 11, edited by C. Domb, Academic Press, 1987.
- [23] Vl. S. Dotsenko, V. A. Fateev, Conformal algebra and multipoint correlation functions in 2D statistical models, *Nucl. Phys.* **B240**, 312 (1984).
- [24] H. Saleur, Lattice models and conformal field theories, *Phys. Rep.* **184**, 177 (1989).
- [25] B. Duplantier, two-dimensional fractal geometry, critical phenomena and conformal invariance, *Phys. Rep.* **184**, 177 (1989).

- [26] C. Vanderzande, *Lattice models of polymers*, Cambridge University Press, 1998.
- [27] A. M. Polyakov, Conformal symmetry of critical fluctuations, JETP Lett. **12**, 381 (1970) [Pisma Zh. Eksp. Teor. Fiz. **12**, 538 (1970)].
- [28] A. A. Belavin, A. M. Polyakov and A. B. Zamolodchikov, Infinite conformal symmetry in two-dimensional quantum field theory, Nucl. Phys. B **241**, 333 (1984).
- [29] L. V. Ahlfors, *Complex analysis*, McGraw-Hill, 1979.
- [30] P. Duren. *Univalent functions*, Springer-Verlag, 1983.
- [31] Sheng Gong, *The Bieberbach conjecture*, Providence, American Mathematical Society, 1999.
- [32] W. Kager, B. Nienhuis, and L. P. Kadanoff, Exact solutions for Loewner evolutions, J. Stat. Phys. **115**, 805 (2004); arXiv: math-ph/0309006.
- [33] M. Bauer, D. Bernard, Conformal field theories of stochastic Loewner evolutions, Commun. Math. Phys. **239**, 493 (2003); arXiv: hep-th/0210015.
- [34] I. Rushkin, P. Oikonomou, L. P. Kadanoff, and I. A. Gruzberg, Stochastic Loewner evolution driven by Lévy processes, J. Stat. Mech., P01001 (2006); arXiv: cond-mat/0509187.
- [35] S. Rohde and O. Schramm, Basic properties of SLE, Ann. of Math. (2) **161**, 883 (2005); arXiv: math.PR/0106036.
- [36] V. Beffara, Hausdorff dimensions for SLE_6 , Ann. Probab. **32**, 2606–2629 (2004); arXiv: math.PR/0204208.
- [37] V. Beffara, The dimension of the SLE curves, arXiv: math.PR/0211322.
- [38] G. F. Lawler, O. Schramm, W. Werner, Conformal invariance of planar loop-erased random walks and uniform spanning trees, Ann. Probab. **32**, 939 (2004); arXiv: math.PR/0112234.
- [39] G. F. Lawler, O. Schramm, W. Werner, On the scaling limit of planar self-avoiding walk, in *Fractal geometry and applications: a jubilee of Benot Mandelbrot, Part 2*, 339, Proc. Sympos. Pure Math., 72, Part 2, Amer. Math. Soc., Providence, RI, 2004; arXiv: math.PR/0204277.

- [40] R. Kenyon, Dominos and the Gaussian free field, *Ann. Probab.* **29**, 1128 (2001); arXiv: math-ph/0002027.
- [41] O. Schramm and S. Sheffield, The harmonic explorer and its convergence to SLE_4 , *Ann. Probab.* **33**, 2127 (2005); arXiv: math.PR/0310210.
- [42] O. Schramm and S. Sheffield, Contour lines of the two-dimensional discrete Gaussian free field, arXiv: math.PR/0605337.
- [43] S. Smirnov, Critical percolation in the plane: conformal invariance, Cardy's formula, scaling limits, *C. R. Acad. Sci. Paris Sér. I Math.* **333**, 239 (2001).
- [44] S. Smirnov, W. Werner, Critical exponents for two-dimensional percolation, *Math. Res. Lett.* **8**, 729, 2001; arXiv: math.PR/0109120.
- [45] B. Øksendal, *Stochastic differential equations*, Springer-Verlag, Berlin, 2003.
- [46] F. C. Klebaner, *Introduction to stochastic calculus with applications*, Imperial College Press, London, 1998.
- [47] G. F. Lawler, O. Schramm, W. Werner, Values of Brownian intersection exponents I: Half-plane exponents, *Acta Math.* **187**, 237 (2001); arXiv: math.PR/9911084.
- [48] G. F. Lawler, O. Schramm, W. Werner, Conformal restriction: the chordal case, *J. Amer. Math. Soc.* **16**, 917 (2003); arXiv: math.PR/0209343.
- [49] R. Friedrich, W. Werner, Conformal fields, restriction properties, degenerate representations and SLE. *C. R. Math. Acad. Sci. Paris* **335**, 947 (2002); arXiv: math.PR/0209382.
- [50] R. Friedrich, W. Werner, Conformal restriction, highest-weight representations and SLE, *Comm. Math. Phys.* **243**, 105–122 (2003); arXiv: math.PR/0301018.
- [51] R. Friedrich, J. Kalkkinen, On conformal field theory and stochastic Loewner evolution, *Nucl. Phys. B* **687**, 279 (2004); arXiv: hep-th/0308020.
- [52] R. Friedrich, On connections of conformal field theory and stochastic Loewner evolution, arXiv: math-ph/0410029.

- [53] M. Bauer, D. Bernard, Conformal transformations and the SLE partition function martingale, *Ann. Henri Poincaré* **5**, 289 (2004); arXiv: math-ph/0305061.
- [54] O. Schramm, A percolation formula, *Elec. Comm. in Probab.* **6**, 115 (2001).
- [55] J. Cardy, Critical percolation in finite geometries, *J. Phys. A: Math. Gen.* **25**, L201 (1992).
- [56] J. Cardy, $SLE(\kappa, \rho)$ and conformal field theory, arXiv: math-ph/0412033;
- [57] R. O. Bauer, R. Friedrich, The correlator toolbox, metrics and moduli, *Nucl. Phys. B* **733**, 91 (2006); arXiv: hep-th/0506046.
- [58] S. Moghimi-Araghi, M. A. Rajabpour, and S. Rouhani, $SLE(\kappa, \rho)$ and boundary Coulomb gas, *Nucl. Phys. B* **740**, 348 (2006); arXiv: hep-th/0508047.
- [59] J. Schulze, Coulomb gas on the half plane, *Nucl. Phys.* **B489**, 580 (1997); **arxiv**
- [60] S. Kawai, Coulomb-gas approach for boundary conformal field theory, *Nucl. Phys. B* **630**, 203 (2002); **arxiv**
- [61] J. Kondev, Loop models, marginally rough interfaces, and the Coulomb gas, *Int. J. Mod. Phys.* **B11**, 153 (1997).
- [62] J. Kondev, C. L. Henley, Kac-Moody symmetries of critical ground states, *Nucl. Phys. B* **464**, 540 (1996).
- [63] J. L. Cardy, Conformal invariance and surface critical behavior, *Nucl. Phys. B* **240**, 514 (1984).
- [64] J. L. Cardy, Boundary conditions, fusion rules and the verlinde formula, *Nucl. Phys. B* **324**, 581 (1989).
- [65] M. Bauer, D. Bernard, SLE, CFT and zig-zag probabilities, arXiv: math-ph/0401019.
- [66] J. B. Garnett, D. E. Marshall, *Harmonic measure*, Cambridge University Press, 2005.

- [67] C. Pommerenke, *Boundary behaviour of conformal maps*, Springer, 1992.
- [68] N. G. Makarov, On the distortion of boundary sets under conformal mappings, *Proc. London Math. Soc.* **51**, 369 (1985).
- [69] N. G. Makarov, Fine structure of harmonic measure, *St. Petersburg Math. J.* **10**, 217 (1999).
- [70] P. Di Francesco, P. Ginsparg, and J. Zinn-Justin, 2D gravity and random matrices, *Phys. Rep.* **254**, 1 (1995); arXiv: hep-th/9306153.
- [71] M. Kontsevich, CFT, SLE and phase boundaries, preprint MPI-2003-60-a, available online at URL <http://www.mpim-bonn.mpg.de/html/preprints/preprints.html>
- [72] M. Bauer, D. Bernard, CFTs of SLEs: the radial case, *Phys. Lett. B* **583**, 324–330 (2004); arXiv: math-ph/0310032.
- [73] M. Bauer, D. Bernard, J. Houdayer, Dipolar stochastic Loewner evolutions, *J. Stat. Mech.* (2005) P03001; arXiv: math-ph/0411038.
- [74] O. Schramm and D. B. Wilson, SLE coordinate changes, *New York J. Math.* **11**, 659 (2005); arXiv: math.PR/0505368.
- [75] R. O. Bauer, Restricting SLE(8/3) to an annulus, arXiv: math.PR/0602391.
- [76] R. O. Bauer and R. Friedrich, Stochastic Loewner evolution in multiply connected domain, *C. R. Acad. Sci. Paris, Ser. I* **339**, 579 (2004); arXiv: math.PR/0408157.
- [77] R. O. Bauer and R. Friedrich, On radial stochastic Loewner evolution in multiply connected domains, arXiv: math.PR/0412060;
- [78] R. O. Bauer and R. Friedrich, On chordal and bilateral SLE in multiply connected domains, arXiv: math.PR/0503178;
- [79] D. Zhan, Stochastic Loewner evolution in doubly connected domains, *Probab. Theory Related Fields* **129**, 340–380 (2004); arXiv: math.PR/0310350;
- [80] G. F. Lawler, Stochastic Loewner evolution, a draft of a contribution on SLE to *Encyclopedia of Mathematical*

Physics to be published by Elsevier, available online at URL <http://www.math.cornell.edu/~lawler/papers.html>

- [81] J. Dubedat, SLE(κ, ρ) martingales and duality, *Ann. Probab.* **33**, 223 (2005); arXiv: math.PR/0303128.
- [82] W. Werner, Girsanov's transformation for SLE(κ, ρ) processes, intersection exponents and hiding exponents, *Ann. Fac. Sci. Toulouse Math.* (6) **13**, 121 (2004); arXiv: math.PR/0302115.
- [83] R. O. Bauer and R. Friedrich, Diffusing polygons and SLE(κ, ρ), arXiv: math.PR/0506062.
- [84] K. Kytölä, On conformal field theory of SLE(κ, ρ), arXiv: math-ph/0504057.
- [85] J. Cardy, Stochastic Loewner evolution and Dyson's circular ensembles, *J. Phys. A: Math. Gen.* **36**, L379 (2003); arXiv: math-ph/0301039.
- [86] J. Dubedat, Commutation relations for SLE, arXiv: math.PR/0411299.
- [87] J. Dubedat, Euler integrals for commuting SLEs, arXiv: math.PR/0507276.
- [88] M. Bauer, D. Bernard, K. Kytölä, Multiple Schramm-Loewner evolutions and statistical mechanics martingales, *J. Stat. Phys.* **120**, 1125 (2005); arXiv: math-ph/0503024.
- [89] K. Kytölä, Virasoro module structure of local martingales for multiple SLEs, arXiv: math-ph/0604047.
- [90] M. J. Kozdron and G. F. Lawler, The configurational measure on mutually avoiding SLE paths, arXiv: math.PR/0605159.
- [91] Qing-Yang Guan, M. Winkel, SLE and alpha-SLE driven by Lévy processes, arXiv: math.PR/0606685.
- [92] J. Rasmussen, On SU(2) Wess-Zumino-Witten models and stochastic evolutions, arXiv: hep-th/0409026.
- [93] E. Bettelheim, I. Gruzberg, A. W. W. Ludwig, P. Wiegmann, Stochastic Loewner evolution for conformal field theories with Lie-group symmetries, *Phys. Rev. Lett.* **95**, 251601 (2005); arXiv: hep-th/0503013.

- [94] D. Bernard, G. Boffetta, A. Celani, G. Falkovich, Conformal invariance in two-dimensional turbulence, *Nature Physics* **2**, 124 (2006).
- [95] C. Amoruso, A. K. Hartmann, M. B. Hastings, and M. A. Moore, Conformal invariance and SLE in two-dimensional Ising spin glasses, arXiv: cond-mat/0601711.
- [96] J. P. Keating, J. Marklof, I. G. Williams, Nodal domain statistics for quantum maps, percolation and SLE, arXiv: nlin.CD/0603068.